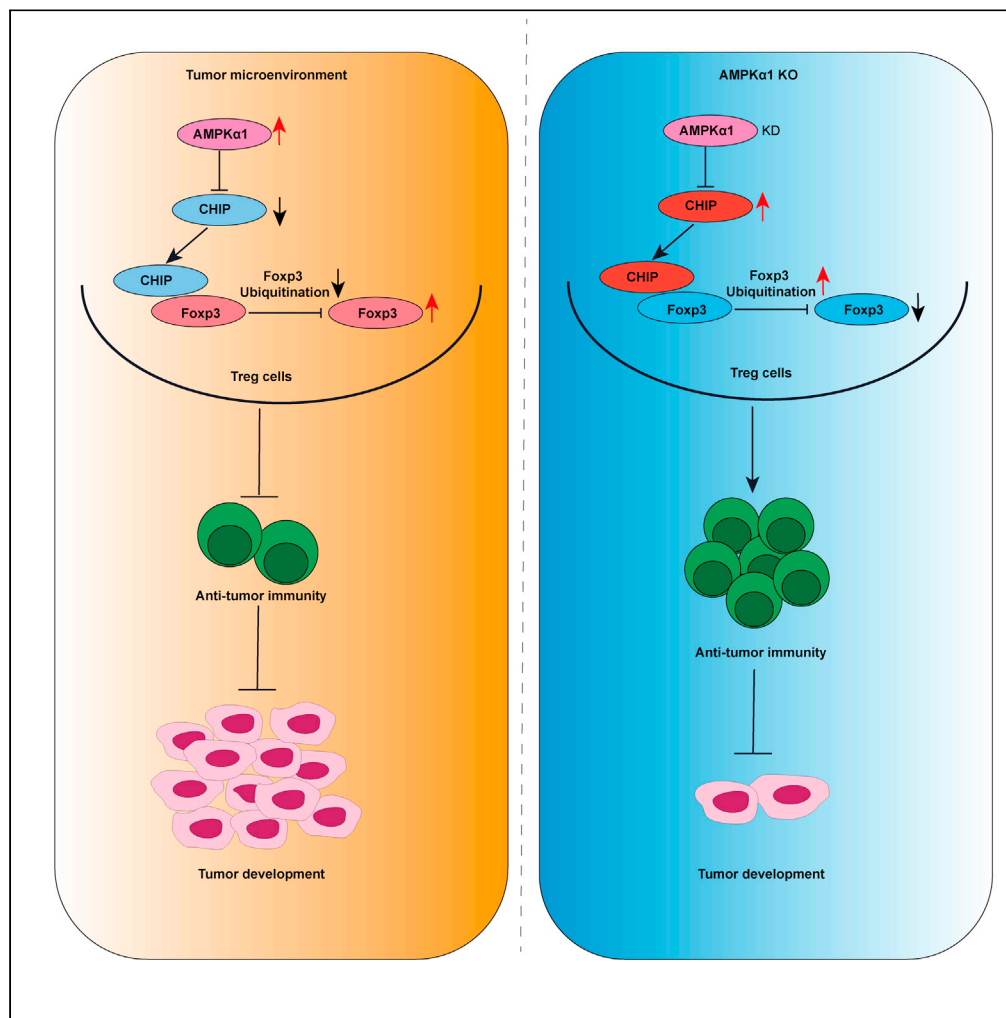


Article

# AMP-activated protein kinase alpha1 promotes tumor development via FOXP3 elevation in tumor-infiltrating Treg cells



Junqing An, Ye Ding, Changjiang Yu, ..., Zhixue Liu, Ping Song, Ming-Hui Zou

psong@gsu.edu (P.S.)  
mzou@gsu.edu (M.-H.Z.)

**Highlights**

AMPKα1 is upregulated in tumor-infiltrated Treg cells

Deficiency of AMPKα1 in Tregs prevents tumor development and promotes antitumor immunity

AMPKα1 regulates Foxp3 protein stability through E3 ligase CHIP



## Article

## AMP-activated protein kinase alpha1 promotes tumor development via FOXP3 elevation in tumor-infiltrating Treg cells

Junqing An,<sup>1</sup> Ye Ding,<sup>1</sup> Changjiang Yu,<sup>1</sup> Jian Li,<sup>1</sup> Shaojin You,<sup>1</sup> Zhixue Liu,<sup>1</sup> Ping Song,<sup>1,\*</sup> and Ming-Hui Zou<sup>1,2,\*</sup>

## SUMMARY

Overwhelming evidence indicates that infiltration of tumors by Treg cells with elevated levels of FOXP3 suppresses the host antitumor immune response. However, the molecular mechanisms that maintain high expression of FOXP3 in tumor-infiltrating Treg cells remain elusive. Here, we report that AMP-activated protein kinase alpha1 (AMPK $\alpha$ 1) enables high FOXP3 expression in tumor-infiltrating Treg cells. Mice with Treg-specific AMPK $\alpha$ 1 deletion showed delayed tumor progression and enhanced antitumor T cell immunity. Further experiments showed that AMPK $\alpha$ 1 maintains the functional integrity of Treg cells and prevents interferon- $\gamma$  production in tumor-infiltrating Treg cells. Mechanistically, AMPK $\alpha$ 1 maintains the protein stability of FOXP3 in Treg cells by downregulating the expression of E3 ligase CHIP (*STUB1*). Our results suggest that AMPK $\alpha$ 1 activation promotes tumor growth by maintaining FOXP3 stability in tumor-infiltrating Treg cells and that selective inhibition of AMPK in Treg cells might be an effective anti-tumor therapy.

## INTRODUCTION

The recognition of tumor antigens by the host immune system promotes antitumor immune responses (Carey et al., 1976). The promotion of tumor-specific T cell responses has been recognized as a promising strategy for cancer therapy (Borst et al., 2018). However, the increased expression of immunosuppressive molecules (PD1/PDL1) and enrichment of immunosuppressive cells (myeloid-derived suppressor cells, tumor-associated macrophages, and regulatory T (Treg) cells) in the tumor microenvironment (TME) limit antitumor immunity and promote tumor immune escape (Han et al., 2020; Kumar et al., 2016; Tanaka and Sakaguchi, 2017; Petty and Yang, 2017). Despite the great progress achieved with immune checkpoint blockers in cancer therapy, the molecular mechanisms that determine the immunosuppressive character of the TME are still not fully understood.

Treg cells are a heterogeneous population of lymphocytes that express the transcription factor Foxp3 and play an essential role in immune balance and tissue homeostasis (Smigiel et al., 2014; Veiga-Parga et al., 2013; Bonney et al., 2015). Stable expression of Foxp3 is required for the development and function of Treg cells, whereas deficiency or mutation of Foxp3 impairs Treg function and causes several autoimmune disorders (Fontenot et al., 2003; Bennett et al., 2001; Bacchetta et al., 2018). In cancers, enrichment of Treg cells in the TME promotes tumor development, invasiveness, and metastasis (Hatzioannou et al., 2017), whereas depletion or inhibition of Treg cells in the TME has found to be a promising strategy for cancer therapy (Xiong et al., 2020; Hatzioannou et al., 2020). In contrast to Treg cells in peripheral blood and other tissues, Treg cells that infiltrate the TME are predominantly Foxp3<sup>high</sup> effector Treg (eTreg) cells, the accumulation of which is linked to poor prognosis of various cancers (Wing et al., 2019). Multiple studies showed that destabilized FOXP3 in Treg cells promotes antitumor immunity and suppresses tumor development (Overacre-Delgoffe and Vignali, 2018; Cortez et al., 2020; Yang et al., 2020). Conversely, elevated Foxp3 expression in tumor-infiltrating Treg cells suppressed the proliferation of effector T cells and promoted gastric cancer progression (Yuan et al., 2010). The molecular mechanism that maintains high Foxp3 expression in tumor-infiltrating Treg cells is still unknown.

AMP-activated kinase (AMPK) is an essential energy sensor activated by the AMP/ATP ratio (Herzig and Shaw, 2018). The activation of AMPK signaling has emerged as a controversial regulator of tumor

<sup>1</sup>Center for Molecular and Translational Medicine, Georgia State University, 157 Decatur Street SE, Atlanta, GA 30303, USA

<sup>2</sup>Lead contact

\*Correspondence: psong@gsu.edu (P.S.), mzou@gsu.edu (M.-H.Z.)

<https://doi.org/10.1016/j.isci.2021.103570>



development (Hardie, 2015). One study showed that AMPK could suppress lymphomagenesis by negatively regulating the Warburg effect (Faubert et al., 2013). Conversely, other studies showed that deletion of AMPK was detrimental to the growth of Kras<sup>G12D</sup>p53<sup>f/f</sup> tumors (Eichner et al., 2019), and inhibition of AMPK activity by Compound C blocked cell cycle progression and prevented B16F1 melanoma growth (Lee et al., 2019). In addition to its effects on cancer cells, AMPK was shown to increase the antitumor activity of tumor-infiltrating CD8<sup>+</sup> T cells by suppressing the transcription of *Pdcd1* (Zhang et al., 2020). The relationship between AMPK and Foxp3 and the role of AMPK in tumor-infiltrating Treg cells remain poorly understood.

We used *in vitro* and *in vivo* experiments to analyze the role of AMPK $\alpha$ 1 in the tumor-promoting effects of Treg cells. Mice with Treg-specific AMPK $\alpha$ 1 deficiency showed increased antitumor immunity and delayed tumor progression. Conditional deletion of AMPK $\alpha$ 1 impaired the immunosuppressive capacity of Treg cells. Furthermore, AMPK $\alpha$ 1 deficiency increased the expression of E3 ligase CHIP and promoted the ubiquitination and proteasomal degradation of FOXP3 in Treg cells. Although further studies are necessary, our results indicate that AMPK suppression in Treg cells might be an effective strategy for cancer immunotherapy.

## RESULTS

### AMPK $\alpha$ 1 is upregulated in tumor-infiltrating Treg cells but is dispensable for T cell development

AMPK is a heterotrimeric complex kinase consisting of  $\alpha$ ,  $\beta$ , and  $\gamma$  subunits, the former of which is responsible for the catalytic activity of the enzyme (Steinberg and Carling, 2019). The two isoforms of AMPK $\alpha$ , AMPK $\alpha$ 1, and AMPK $\alpha$ 2, are encoded by the *Prkaa1* and *Prkaa2* genes, respectively (Steinberg and Carling, 2019). AMPK $\alpha$ 1 is the predominant isoform in T cells, which also express AMPK $\alpha$ 2 but at lower levels (Tamas et al., 2006; Mayer et al., 2008). To explore the regulation and function of AMPK signaling in tumor-infiltrating Treg cells, we monitored AMPK $\alpha$ 1 expression in Treg cells from tumors and spleens of mice bearing B16F10 melanoma tumors. Flow cytometry revealed that the frequency of Treg cells was higher in the TME than in the spleen (Figure 1A) and that the AMPK $\alpha$ 1 expression level was higher in Treg cells from tumors than in Treg cells from the spleen (Figure 1B).

To further examine the role of AMPK $\alpha$ 1 in Treg cells, we generated Treg-specific AMPK $\alpha$ 1-deficiency mice (*Prkaa1<sup>fl/fl</sup>Foxp3<sup>Cre/YFP</sup>*, hereafter referred to as AMPK $\alpha$ 1<sup>Treg<sup>-/-</sup>) by crossing mice bearing loxp-flanked *Prkaa1* alleles with Foxp3-Cre/YFP mice (littermate controls *Prkaa1<sup>+/+</sup>Foxp3<sup>Cre/YFP</sup>* referred to as AMPK $\alpha$ 1<sup>Treg<sup>+/+</sup>). We then confirmed that the AMPK $\alpha$ 1 protein level was deleted in Foxp3-YFP<sup>+</sup> Treg cells but not in CD4<sup>+</sup>Foxp3-YFP<sup>-</sup> Tconv cells (T conventional cells) from the AMPK $\alpha$ 1<sup>Treg<sup>-/-</sup> mice (Figure S1A). Flow cytometry analysis showed no difference in the frequencies of Treg cells and other T cell phenotypes in the thymus between the AMPK $\alpha$ 1<sup>Treg<sup>-/-</sup> mice and the AMPK $\alpha$ 1<sup>Treg<sup>+/+</sup> mice (Figure S1B–S1D), implying that AMPK $\alpha$ 1 plays a dispensable role in the development of Treg cells.</sup></sup></sup></sup></sup>

### AMPK deletion in Treg cells suppresses tumor progression

We challenged AMPK $\alpha$ 1<sup>Treg<sup>-/-</sup> mice and AMPK $\alpha$ 1<sup>Treg<sup>+/+</sup> mice with B16F10 melanoma cells to explore how AMPK $\alpha$ 1 expression in Treg cells affects tumor development. Compared with the AMPK $\alpha$ 1<sup>Treg<sup>+/+</sup> mice, the AMPK $\alpha$ 1<sup>Treg<sup>-/-</sup> mice showed decreased tumor size (Figure 1C). Furthermore, the growth of the melanoma cells was largely attenuated in the AMPK $\alpha$ 1<sup>Treg<sup>-/-</sup> mice relative to that in the AMPK $\alpha$ 1<sup>Treg<sup>+/+</sup> mice (Figure 1D). Moreover, AMPK $\alpha$ 1<sup>Treg<sup>-/-</sup> mice had lower tumor weight (Figure 1E), less tumor blood vessel formation (Figure 1F), and lower frequencies of Ki-67<sup>+</sup> proliferating cells in their tumors (Figure 1G). Similarly, AMPK $\alpha$ 1<sup>Treg<sup>-/-</sup> mice showed decreased tumor sizes and delayed tumor progression when compared with AMPK $\alpha$ 1<sup>Treg<sup>+/+</sup> mice after implantation with Lewis lung carcinoma cells (LLCs; Figure S2A–S2C). These findings indicate that deficiency of AMPK $\alpha$ 1 in Treg cells impairs tumor progression in mice.</sup></sup></sup></sup></sup></sup></sup></sup></sup>

### AMPK $\alpha$ 1 deficiency in Treg cells promotes antitumor T cell responses

Histological analysis revealed that tumor tissues from AMPK $\alpha$ 1<sup>Treg<sup>-/-</sup> mice had more inflammatory cell infiltration than those from AMPK $\alpha$ 1<sup>Treg<sup>+/+</sup> mice (Figure S3A). Further analysis showed the tumors from the AMPK $\alpha$ 1<sup>Treg<sup>-/-</sup> mice had more CD3<sup>+</sup>, CD4<sup>+</sup>, and CD8<sup>+</sup> T cell infiltration than the tumors from the AMPK $\alpha$ 1<sup>Treg<sup>+/+</sup> mice (Figures 2A and 2B); however, the frequency of tumor-infiltrating B cells was</sup></sup></sup></sup>

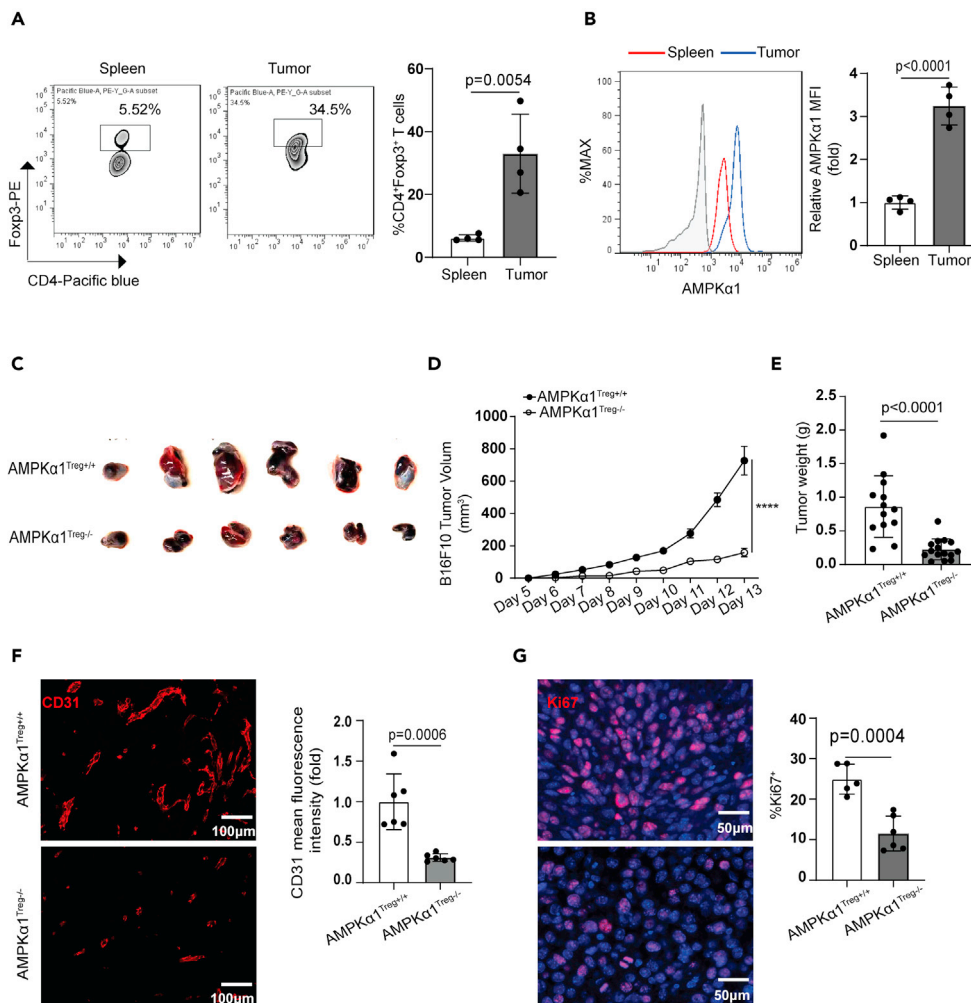


**Figure 1. AMPK $\alpha$ 1 is upregulated in tumor-infiltrating Tregs and promotes tumor development**

(A) Representative flow cytometry images and quantification of CD4<sup>+</sup>Foxp3<sup>+</sup> frequency in mouse spleens and tumors on day 10 after B16F10 melanoma implantation (n = 4 in each group; data are presented as individual values and mean  $\pm$  SD and analyzed by Student's t test).

(B) Representative flow cytometry images and quantification of AMPK $\alpha$ 1 mean fluorescence intensity (MFI) in Treg cells from mouse spleens and tumors (n = 4 in each group; data are presented as individual values and mean  $\pm$  SD and analyzed by Student's t test).

(C) Representative images of tumors from AMPK $\alpha$ 1<sup>Treg+/+</sup> and AMPK $\alpha$ 1<sup>Treg-/-</sup> mice on day 13 after implantation with B16F10 cells.

(D) Tumor volume in AMPK $\alpha$ 1<sup>Treg+/+</sup> and AMPK $\alpha$ 1<sup>Treg-/-</sup> mice after implantation with B16F10 cells (n = 13 in AMPK $\alpha$ 1<sup>Treg+/+</sup> group and n = 15 in AMPK $\alpha$ 1<sup>Treg-/-</sup> group; data are presented as mean  $\pm$  SEM and analyzed by two-way ANOVA).

(E) Tumor weight in AMPK $\alpha$ 1<sup>Treg+/+</sup> and AMPK $\alpha$ 1<sup>Treg-/-</sup> mice on day-13 after implantation with B16F10 cells (n = 13 in AMPK $\alpha$ 1<sup>Treg+/+</sup> group and n = 15 in AMPK $\alpha$ 1<sup>Treg-/-</sup> group; data are presented as individual values and mean  $\pm$  SD and analyzed by Student's t test).

(F) Representative images of immunofluorescence and quantification of CD31 intensity in tumors from AMPK $\alpha$ 1<sup>Treg+/+</sup> and AMPK $\alpha$ 1<sup>Treg-/-</sup> mice on day 10 after implantation with B16F10 cells (n = 6 in each group; data are presented as individual values and mean  $\pm$  SD and analyzed by Student's t test). Three or more fields per tumor were quantified. Scale bar: 100  $\mu$ m.

(G) Representative images of immunofluorescence and percentage of Ki67<sup>+</sup> cells in tumors from AMPK $\alpha$ 1<sup>Treg+/+</sup> and AMPK $\alpha$ 1<sup>Treg-/-</sup> mice on day 10 after implantation with B16F10 cells (n = 5 in AMPK $\alpha$ 1<sup>Treg+/+</sup> group and n = 6 in AMPK $\alpha$ 1<sup>Treg-/-</sup> group; data are presented as individual values and mean  $\pm$  SD and analyzed by Student's t test). Three or more fields per tumor were quantified. Scale bar: 50  $\mu$ m.

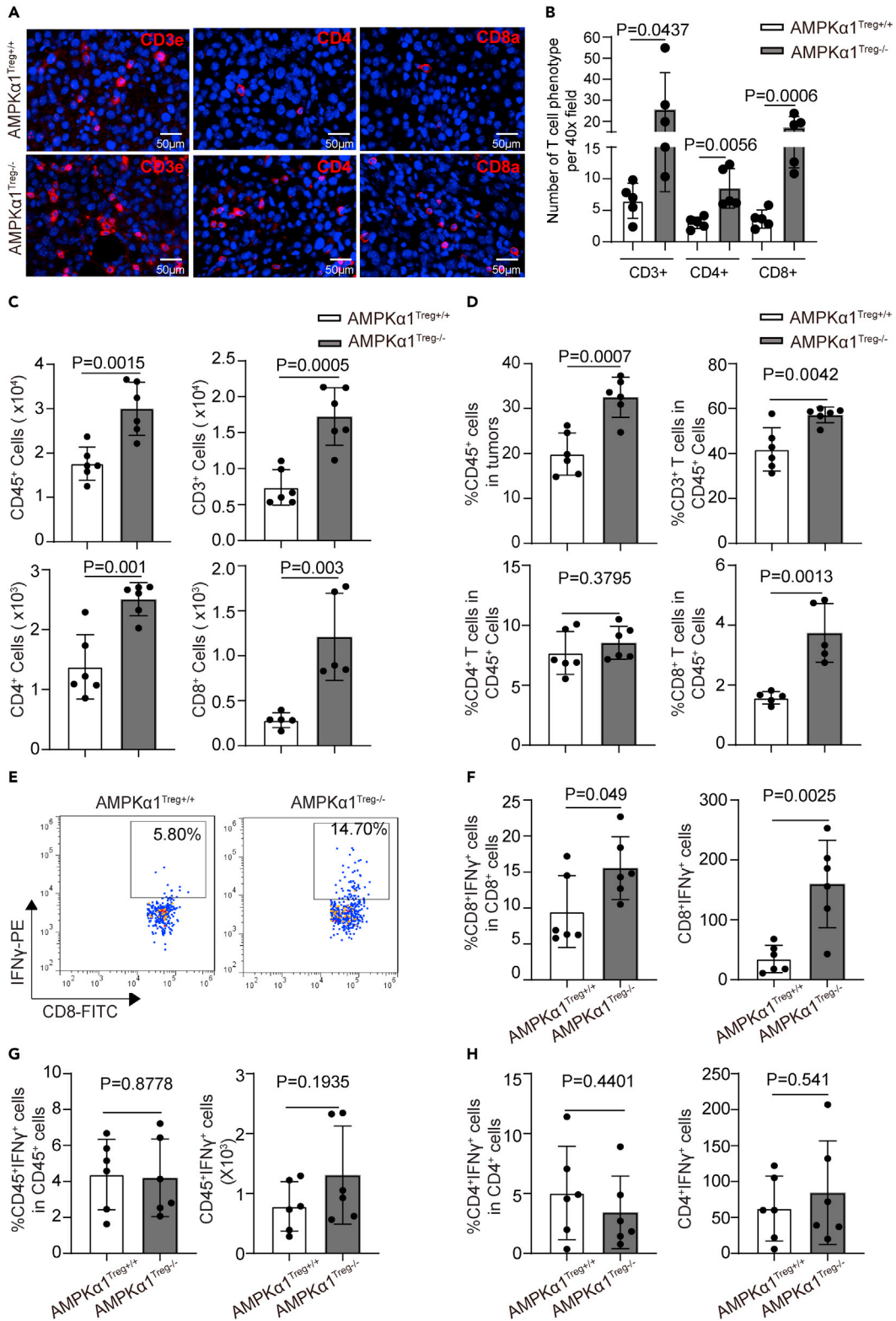


**Figure 2. Treg-specific AMPK $\alpha$ 1 deficient mice show increased antitumor immunity**

- (A) Representative immunofluorescence staining images of CD3e, CD4, and CD8a in tumor sections from AMPK $\alpha$ 1<sup>Treg+/+</sup> and AMPK $\alpha$ 1<sup>Treg-/-</sup> mice. Scale bar: 50  $\mu$ m.
- (B) Cell numbers of CD3<sup>+</sup>, CD4<sup>+</sup>, and CD8<sup>+</sup> T cells per 40 $\times$  field in tumor sections from AMPK $\alpha$ 1<sup>Treg+/+</sup> and AMPK $\alpha$ 1<sup>Treg-/-</sup> mice (n = 5 in each group; data are presented as individual values and mean  $\pm$  SD and analyzed by Student's t test). Five or more fields per tumor were quantified.
- (C) Numbers of CD45<sup>+</sup> (n = 6), CD3<sup>+</sup> (n = 6), CD4<sup>+</sup> (n = 6), and CD8<sup>+</sup> (n = 5) T cells per 1  $\times$  10<sup>6</sup> tumor cells from day-13 tumor tissues of AMPK $\alpha$ 1<sup>Treg+/+</sup> and AMPK $\alpha$ 1<sup>Treg-/-</sup> mice measured by flow cytometry (data are presented as individual values and mean  $\pm$  SD and analyzed by Student's t test).
- (D) Proportions of CD45<sup>+</sup> (n = 6), CD3<sup>+</sup> (n = 6), CD4<sup>+</sup> (n = 6), and CD8<sup>+</sup> (n = 5) T cells in day-13 tumor tissues of AMPK $\alpha$ 1<sup>Treg+/+</sup> and AMPK $\alpha$ 1<sup>Treg-/-</sup> mice analyzed by flow cytometry (data are presented as individual values and mean  $\pm$  SD and analyzed by Student's t test).
- (E) Representative FACS images of IFN- $\gamma$ -producing CD8<sup>+</sup> cells from day-13 tumor tissues of AMPK $\alpha$ 1<sup>Treg+/+</sup> and AMPK $\alpha$ 1<sup>Treg-/-</sup> mice.
- (F) Frequency and numbers of IFN- $\gamma$ -producing CD8<sup>+</sup> cells per 1  $\times$  10<sup>6</sup> tumor cells from tumor tissues of AMPK $\alpha$ 1<sup>Treg+/+</sup> and AMPK $\alpha$ 1<sup>Treg-/-</sup> mice (n = 6 in each group; data are presented as individual values and mean  $\pm$  SD and analyzed by Student's t test).
- (G) Frequency and numbers of IFN- $\gamma$ -producing CD45<sup>+</sup> cells per 1  $\times$  10<sup>6</sup> tumor cells from tumor tissues of AMPK $\alpha$ 1<sup>Treg+/+</sup> and AMPK $\alpha$ 1<sup>Treg-/-</sup> mice (n = 6 in each group; data are presented as individual values and mean  $\pm$  SD and analyzed by Student's t test).
- (H) Frequency and numbers of IFN- $\gamma$ -producing CD4<sup>+</sup> cells per 1  $\times$  10<sup>6</sup> tumor cells from tumor tissues of AMPK $\alpha$ 1<sup>Treg+/+</sup> and AMPK $\alpha$ 1<sup>Treg-/-</sup> mice (n = 6 in each group; data are presented as individual values and mean  $\pm$  SD and analyzed by Student's t test).

comparable between the two mouse strains (Figure S3B). These data indicate an enhanced antitumor immunity in the AMPK $\alpha$ 1<sup>Treg-/-</sup> mice.

Next, we performed flow cytometry analysis of the tumors to further explore the antitumor effects of AMPK $\alpha$ 1 deletion in Treg cells (Figure S3C). Compared with the tumors from the AMPK $\alpha$ 1<sup>Treg+/+</sup> mice, the tumors from the AMPK $\alpha$ 1<sup>Treg-/-</sup> mice had increased numbers of CD45<sup>+</sup> leukocytes, CD3<sup>+</sup> T cells, CD4<sup>+</sup> T cells, and CD8<sup>+</sup> T cells (Figure 2C). Meanwhile, the proportions of CD45<sup>+</sup> cells in tumors and the frequency of CD3<sup>+</sup> and CD8<sup>+</sup> T cells in CD45<sup>+</sup> cells significantly increased in tumor tissues from AMPK $\alpha$ 1<sup>Treg-/-</sup> mice (Figure 2D). The expression of IFN- $\gamma$ , an important cytotoxic cytokine, by tumor-infiltrating CD8<sup>+</sup> T cells was also higher in AMPK $\alpha$ 1<sup>Treg-/-</sup> mice than that in AMPK $\alpha$ 1<sup>Treg+/+</sup> mice (Figures 2E and 2F). However, the frequency and numbers of tumor-infiltrating CD45<sup>+</sup>IFN $\gamma$ <sup>+</sup> and CD4<sup>+</sup>IFN $\gamma$ <sup>+</sup> T cells were comparable between AMPK $\alpha$ 1<sup>Treg+/+</sup> mice and AMPK $\alpha$ 1<sup>Treg-/-</sup> mice (Figures 2G and 2H). These findings suggest that the absence of AMPK $\alpha$ 1 in Treg cells promotes CD8<sup>+</sup> T cells mediated antitumor immunity.

**AMPK $\alpha$ 1-deficient Treg cells present a 'fragile' phenotype in TME.**

Our observations of increased antitumor immunity in AMPK $\alpha$ 1<sup>Treg-/-</sup> mice led us to assess possible changes in the Treg populations. Intratumoral Treg cells can present a 'fragile' phenotype, marked by aberrant IFN- $\gamma$  expression but loss of Treg signature genes, was shown to promote more efficient antitumor immunity (Lim et al., 2021; Overacre-Delgoffe et al., 2017). Next, we tested whether AMPK could influence the formation of 'fragile' Treg cells in TME. Several cell surface markers are related to the immunosuppressive function of Treg cells and have been exploited as cancer therapeutic targets (Ohue and Nishikawa, 2019). Analysis of these cell surface markers revealed a decrease in CD25, CTLA-4, and PD1 expression in AMPK $\alpha$ 1-deficient Treg cells in TME compared with that in wild-type (WT) Treg cells (Figures 3A–3C). In addition, both the frequency and mean fluorescence intensities (MFIs) of IL-10, an inhibitory cytokine expressed by Treg cells, were decreased in tumor infiltrating CD4<sup>+</sup>Foxp3-YFP<sup>+</sup> Treg cells after AMPK $\alpha$ 1 deletion (Figures 3D and 3E). These data indicate that the functional integrity of Treg cells was compromised after AMPK $\alpha$ 1 deficiency in TME. Through analysis of the expression of IFN- $\gamma$  in tumor infiltrating Treg cells, we found an increased frequency of IFN- $\gamma$ <sup>+</sup> Treg cells in tumors from AMPK $\alpha$ 1<sup>Treg-/-</sup> mice compared with controls (Figure 3F). Meanwhile, the expression of IFN- $\gamma$  in tumor-Treg cells also showed an increase in AMPK $\alpha$ 1<sup>Treg-/-</sup> mice (Figure 3G). Overall, these data point toward an essential role of AMPK $\alpha$ 1 in maintaining the function profile of Treg cells in TME and preventing the induction of fragile Treg cells.

**AMPK $\alpha$ 1 maintains FOXP3 expression in Treg cells**

As a key transcriptional factor, Foxp3 controls the development and functional integrity of Treg cells (Fontenot et al., 2003). Unstable FOXP3 expression promotes IFN- $\gamma$  transcription in Treg cells (Yang et al., 2020). Immunofluorescence staining of FOXP3 showed similar numbers of Foxp3<sup>+</sup> cells in tumor sections from AMPK $\alpha$ 1<sup>Treg+/+</sup> and AMPK $\alpha$ 1<sup>Treg-/-</sup> mice (Figure 4A). Nonetheless, the FOXP3 fluorescence intensity in Foxp3<sup>+</sup> cells from the tumors of AMPK $\alpha$ 1<sup>Treg-/-</sup> mice was lower than that from the tumors of AMPK $\alpha$ 1<sup>Treg+/+</sup> mice (Figures 4A and 4B), indicating that AMPK $\alpha$ 1 deficiency decreases FOXP3 protein level in the Treg cells during tumor development.

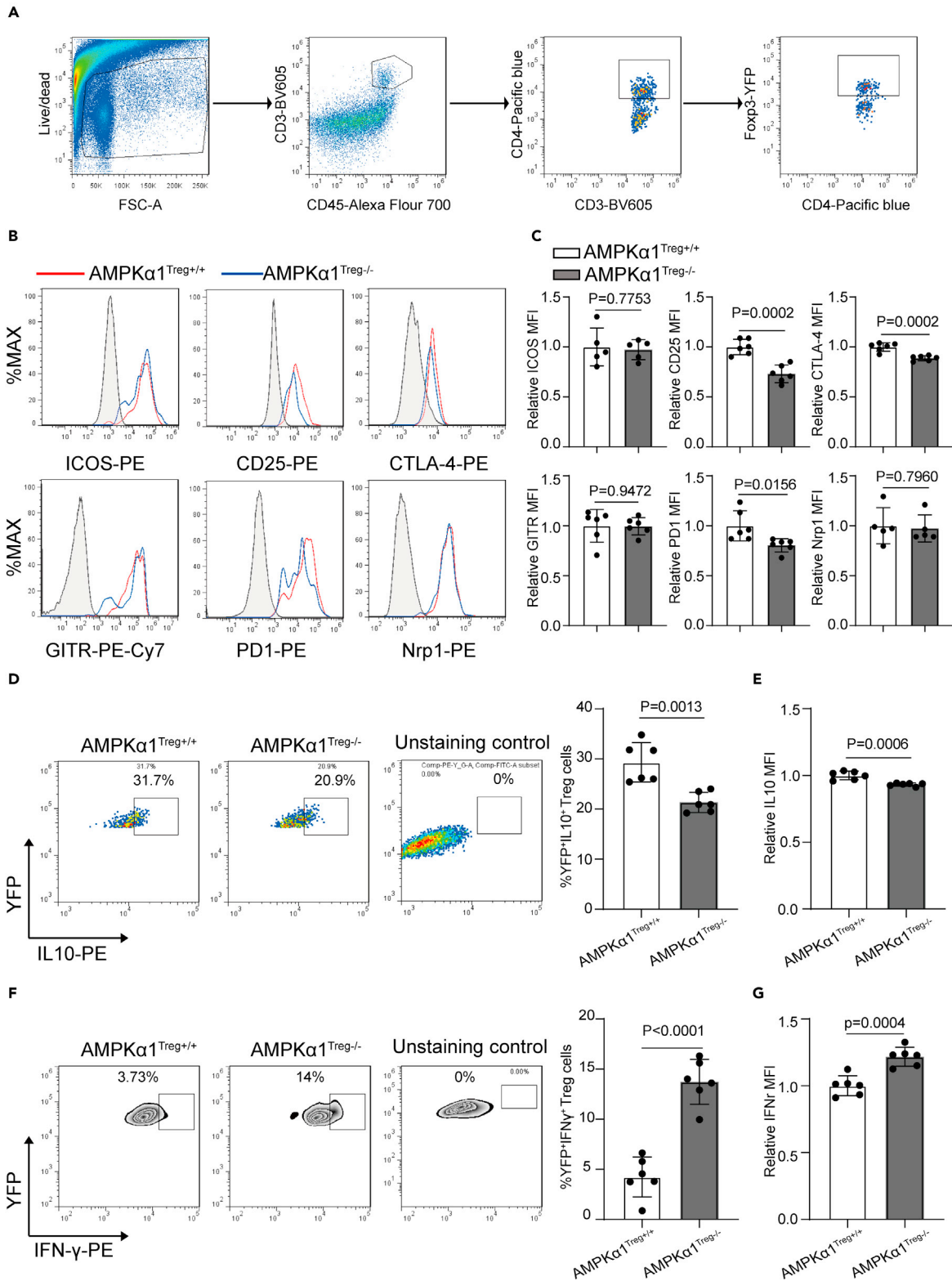


**Figure 3. AMPK $\alpha$ 1-deficient Treg cells present a 'fragile' phenotype in TME**

(A) Gating strategy of CD4<sup>+</sup>YFP<sup>+</sup> Treg cells from tumor tissues.

(B) Representative FACS images of ICOS, CD25, CTLA-4, GITR, PD1, and Nrp1 expression on CD4<sup>+</sup>Foxp3-YFP<sup>+</sup> Treg cells from day 13 tumor tissues of AMPK $\alpha$ 1<sup>Treg+/+</sup> and AMPK $\alpha$ 1<sup>Treg-/-</sup> mice.

(C) Relative MFI of cell surface ICOS (n = 5), CD25 (n = 6), CTLA-4 (n = 6), GITR (n = 6), PD1 (n = 6) and Nrp1 (n = 5) on CD4<sup>+</sup>Foxp3-YFP<sup>+</sup> Treg cells from day 13 tumor tissues of AMPK $\alpha$ 1<sup>Treg+/+</sup> and AMPK $\alpha$ 1<sup>Treg-/-</sup> mice. (Data are presented as individual values and mean  $\pm$  SD and analyzed by Student's t test).

(D) Representative FACS images and frequency of YFP<sup>+</sup>IL-10<sup>+</sup> Treg cells in CD4<sup>+</sup>Foxp3-YFP<sup>+</sup> Treg cells from day 13 tumor tissues of AMPK $\alpha$ 1<sup>Treg+/+</sup> and AMPK $\alpha$ 1<sup>Treg-/-</sup> mice. (n = 6 in each group, data are presented as individual values and mean  $\pm$  SD and analyzed by Student's t test).

(E) Relative MFI of IL-10 in CD4<sup>+</sup>Foxp3-YFP<sup>+</sup> Treg cells from day 13 tumor tissues of AMPK $\alpha$ 1<sup>Treg+/+</sup> and AMPK $\alpha$ 1<sup>Treg-/-</sup> mice. (n = 6 in each group, data are presented as individual values and mean  $\pm$  SD).

(F) Representative FACS images and frequency of YFP<sup>+</sup>IFN- $\gamma$ <sup>+</sup> Treg cells in CD4<sup>+</sup>Foxp3-YFP<sup>+</sup> Treg cells from day 13 tumor tissues of AMPK $\alpha$ 1<sup>Treg+/+</sup> and AMPK $\alpha$ 1<sup>Treg-/-</sup> mice. (n = 6 in each group, data are presented as individual values and mean  $\pm$  SD and analyzed by Student's t test).

(G) Relative MFI of IFN- $\gamma$  in CD4<sup>+</sup>Foxp3-YFP<sup>+</sup> Treg cells from day 13 tumor tissues of AMPK $\alpha$ 1<sup>Treg+/+</sup> and AMPK $\alpha$ 1<sup>Treg-/-</sup> mice. (n = 6 in each group, data are presented as individual values and mean  $\pm$  SD and analyzed by Student's t test).

To establish the role of AMPK in Foxp3 regulation in Treg cells, we analyze the expression of yellow fluorescent protein (YFP), a reporter of transcriptional induction of Foxp3. We found that deficiency of AMPK $\alpha$ 1 has a mild effect on the frequency of CD4<sup>+</sup>YFP<sup>+</sup> cells and the MFIs of YFP, but significantly decreased FOXP3 expression in tumor infiltrated CD4<sup>+</sup>YFP<sup>+</sup> Treg cells (Figures 4C and 4D). These data suggest that deletion of AMPK $\alpha$ 1 does not affect the induction of the *Foxp3* gene, but it compromises the expression of the FOXP3 protein after tumor implantation.

To test whether this effect also happened in steady state, we used both GFP antibody (YFP signal can be detected by GFP antibody) and Foxp3 antibody to analyze the CD4<sup>+</sup>YFP<sup>+</sup> and CD4<sup>+</sup>Foxp3<sup>+</sup> Treg frequency, respectively, in the spleen of AMPK $\alpha$ 1<sup>Treg+/+</sup> and AMPK $\alpha$ 1<sup>Treg-/-</sup> mice without tumor implantation. Both the frequency of CD4<sup>+</sup>YFP<sup>+</sup> Treg cells and expression of YFP were comparable between both strains, whereas the frequency of CD4<sup>+</sup>Foxp3<sup>+</sup> Treg cells and expression of Foxp3 significantly decreased in AMPK $\alpha$ 1<sup>Treg-/-</sup> mice (Figures 4E–4H). Therefore, both in TME and stable state, AMPK $\alpha$ 1 is required for Foxp3 protein level, but it does not affect the survival/proportion of Treg cells.

**Deficiency of AMPK $\alpha$ 1 impairs FOXP3 protein stability**

T cell receptor (TCR) signaling is required for Foxp3 expression, either through induction of *Foxp3* transcription or through post-translational modification (Ono, 2020). Activation of TCR signaling by CD3/CD28 Dynabeads promoted AMPK $\alpha$ 1 expression in AMPK $\alpha$ 1-sufficient (WT) Treg cells but not in AMPK $\alpha$ 1-deficient (KO) Treg cells (Figures 5A and 5B). Although FOXP3 expression was also increased in both types of Treg cells after CD3/CD28 treatment, the folds of increase in the AMPK $\alpha$ 1-deficient (KO) Treg cells were smaller compared to the AMPK $\alpha$ 1-sufficient (WT) Treg cells (Figures 5C and 5D). These data suggest that AMPK $\alpha$ 1 is partially required for TCR-induced FOXP3 upregulation.

To further investigate the intracellular mechanism by how AMPK $\alpha$ 1 regulates Foxp3 expression in Treg cells, we isolated Treg cells from AMPK $\alpha$ 1<sup>Treg+/+</sup> and AMPK $\alpha$ 1<sup>Treg-/-</sup> mice and compared the protein and mRNA levels of Foxp3. We found that the FOXP3 protein level was much lower in the AMPK $\alpha$ 1<sup>-/-</sup> Treg cells than those in the AMPK $\alpha$ 1<sup>+/+</sup> Treg cells (Figure 5E), whereas the *Foxp3* mRNA level was similar (Figure 5F).

Next, we asked whether AMPK regulates FOXP3 protein stability. We transfected human embryonic kidney (HEK) 293 cells with Flag-Foxp3 plasmid together with AMPK $\alpha$ 1 plasmid or AMPK $\alpha$ 1 siRNA (Figures 5G and 5H). We found that AMPK $\alpha$ 1 overexpression prevented cycloheximide (CHX)-induced reduction of FOXP3 levels (Figure 5G), whereas AMPK $\alpha$ 1 silencing decreased the protein stability of FOXP3 (Figure 5H). These data suggest that AMPK $\alpha$ 1 stabilizes the FOXP3 protein through post-translational modification.

**Deficiency of AMPK $\alpha$ 1 promotes FOXP3 degradation through E3 ligase CHIP**

The stability of FOXP3 is tightly regulated by proteasomal degradation (Barbi et al., 2015). We therefore asked whether the reduced protein level of FOXP3 in AMPK $\alpha$ 1-deficient Treg cells could be recovered by blocking proteasomal degradation. As shown in Figure 6A, treatment with the proteasome inhibitor MG132 normalized Foxp3 levels in Treg cells from AMPK $\alpha$ 1<sup>Treg-/-</sup> mice. Because post-translational ubiquitination of FOXP3 affects FOXP3 stability and Treg function (Barbi et al., 2015), we next determined whether AMPK $\alpha$ 1 regulates FOXP3 ubiquitination. To this end, Flag-Foxp3 plasmids were transfected into HEK

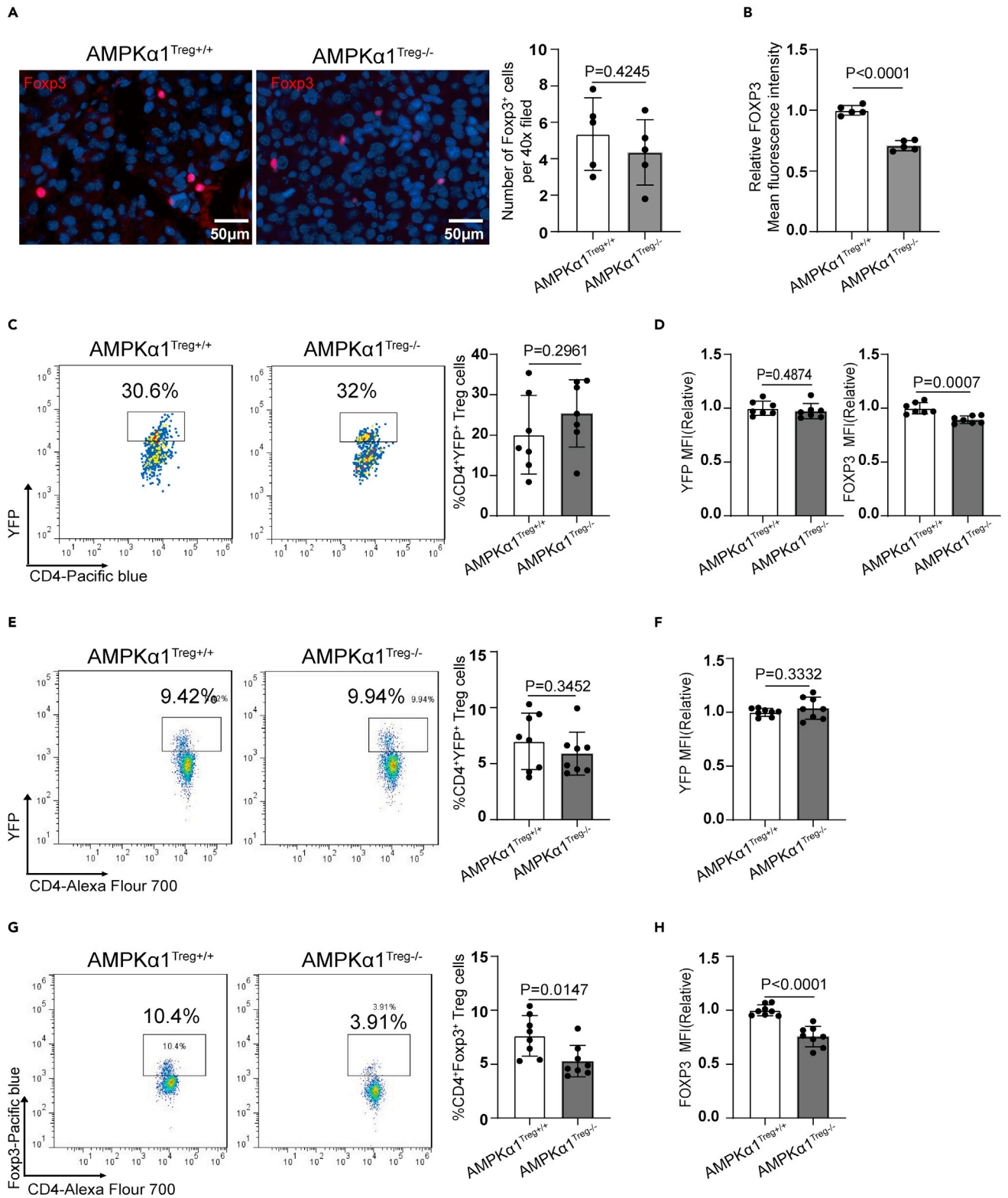


**Figure 4. AMPK $\alpha$ 1 deficiency impairs FOXP3 expression in Treg cells**

(A) Representative immunofluorescence images of FOXP3 and quantification of Foxp3<sup>+</sup> cell numbers on tumor sections from AMPK $\alpha$ 1<sup>Treg+/+</sup> and AMPK $\alpha$ 1<sup>Treg-/-</sup> mice (n = 5 in each group; data are presented as individual values and mean  $\pm$  SD and analyzed by Student's t test). Five or more fields per tumor were quantified. Scale bar: 50  $\mu$ m.

(B) Quantification of FOXP3 fluorescence intensity in Foxp3<sup>+</sup> cells. (n = 5 in each group; data are presented as individual values and mean  $\pm$  SD and analyzed by Student's t test). Five or more fields per tumor were quantified.

(C) Representative FACS images and percentage of CD4<sup>+</sup>YFP<sup>+</sup> Treg cells in day-13 tumor tissues of AMPK $\alpha$ 1<sup>Treg+/+</sup> and AMPK $\alpha$ 1<sup>Treg-/-</sup> mice (n = 7 in each group; data are presented as individual values and mean  $\pm$  SD and analyzed by Student's t test).

(D) Relative MFI of YFP and FOXP3 in tumor infiltrated CD4<sup>+</sup>YFP<sup>+</sup> Treg cells of AMPK $\alpha$ 1<sup>Treg+/+</sup> and AMPK $\alpha$ 1<sup>Treg-/-</sup> mice (n = 7 in each group; data are presented as individual values and mean  $\pm$  SD and analyzed by Student's t test).

(E) Representative FACS images and frequency of CD4<sup>+</sup>YFP<sup>+</sup> Treg cells in the spleens of AMPK $\alpha$ 1<sup>Treg+/+</sup> and AMPK $\alpha$ 1<sup>Treg-/-</sup> mice under steady state (n = 8 in each group; data are presented as individual values and mean  $\pm$  SD and analyzed by Student's t test).

(F) Relative MFI of YFP in CD4<sup>+</sup>YFP<sup>+</sup> Treg cells from AMPK $\alpha$ 1<sup>Treg+/+</sup> and AMPK $\alpha$ 1<sup>Treg-/-</sup> mice under steady state (n = 8 in each group; data are presented as individual values and mean  $\pm$  SD and analyzed by Student's t test).

(G) Representative FACS images and frequency of CD4<sup>+</sup>Foxp3<sup>+</sup> Treg cells in the spleens of AMPK $\alpha$ 1<sup>Treg+/+</sup> and AMPK $\alpha$ 1<sup>Treg-/-</sup> mice under steady state (n = 8 in each group; data are presented as individual values and mean  $\pm$  SD and analyzed by Student's t test).

(H) Relative MFI of FOXP3 in Treg cells from AMPK $\alpha$ 1<sup>Treg+/+</sup> and AMPK $\alpha$ 1<sup>Treg-/-</sup> mice under steady state (n = 8 in each group; data are presented as individual values and mean  $\pm$  SD and analyzed by Student's t test).

293T cells together with either control siRNA or AMPK $\alpha$ 1 siRNA. We then treated the cells with MG132 and performed Flag-Foxp3 pull-down and immunoblot to assess the ubiquitination of Foxp3. We found that ubiquitination of FOXP3 was increased when AMPK $\alpha$ 1 was knocked down (Figure 6B). These results imply that deficiency of AMPK $\alpha$ 1 promotes Foxp3 degradation through polyubiquitination-mediated proteasomal degradation, which results in a decrease of Foxp3 levels in Treg cells.

Finally, we investigated how AMPK regulates FOXP3 ubiquitination and degradation. The polyubiquitination and degradation of FOXP3 are controlled by E3 ligase CHIP (*STUB1*) and deubiquitinase USP7 (Chen et al., 2013; van Loosdregt et al., 2013). We found that the expression of deubiquitinase USP7 was comparable between AMPK $\alpha$ 1-sufficient and AMPK $\alpha$ 1-deficient Treg cells (Figure 6C); however, both the protein and mRNA level of CHIP were higher in AMPK $\alpha$ 1-deficient Treg cells than those in AMPK $\alpha$ 1-sufficient Treg cells (Figures 6D and 6E). We observed a similar effect in tumor infiltrating Treg cells, which showed increased CHIP expression after AMPK $\alpha$ 1 deletion (Figure S4). Furthermore, CHIP knockdown by shCHIP lentivirus partially recovered the reduced Foxp3 expression in AMPK $\alpha$ 1-deficient Treg cells (Figures 6F and 6G). These results indicated that CHIP is partially responsible for the modulation of Foxp3 protein stability by AMPK $\alpha$ 1.

**DISCUSSION**

Accumulating evidence suggest that cell-intrinsic molecules that potentiate Foxp3 expression in tumor-infiltrating Treg cells can provide new targets for cancer therapy (Xiong et al., 2020; Hatzioannou et al., 2020; Cortez et al., 2020). In this study, we found that AMPK $\alpha$ 1 is highly expressed in tumor-infiltrating Treg cells and is indispensable in these cells for FOXP3 expression and functional integrity of Treg cells in TME. Tumor-exposed Treg-specific AMPK $\alpha$ 1 deficiency mice exhibited increased numbers of tumor-infiltrating T cells and more efficient antitumor immunity. AMPK $\alpha$ 1 maintained the protein stability of FOXP3 while not affecting the transcription of *Foxp3* in Treg cells. Furthermore, increased E3 ligase CHIP (*STUB1*) expression in AMPK $\alpha$ 1-deficient Treg cells promotes the ubiquitination and proteasomal degradation of FOXP3, while decreasing FOXP3 levels in Treg cells.

AMPK signaling activates both antitumor and protumor immune responses in the TME. Activation of AMPK by its agonist, metformin, promotes the phosphorylation and degradation of PD-L1, which promotes antitumor immunity (Cha et al., 2018). Conversely, inhibition of AMPK activity in tumor-bearing mice, as well as conditional deletion of AMPK $\alpha$ 1 in myeloid cells, improves protective T cell immunity by suppressing the immunoregulatory function of myeloid-derived suppressor cells (Trillo-Tinoco et al., 2019). In addition, AMPK inhibition reduces immunosuppressive phenotypes in tumor-associated macrophages and unleashes an antitumor effector T cell response (Xu et al., 2018; Wang et al., 2019). Thus, the modulation of AMPK has combined effects in different cell populations within the TME. The nutrient sparse, hypoxic, and acidic environment of tumor tissues negatively affect T effector cell function while supporting Treg cell function (Watson et al., 2021; Zappasodi et al., 2021). AMPK is upregulated and activated in the hypoxic and nutrient-limited TME (Gutierrez-Salmeron et al., 2020; Hao et al., 2015); however, the regulation and role of

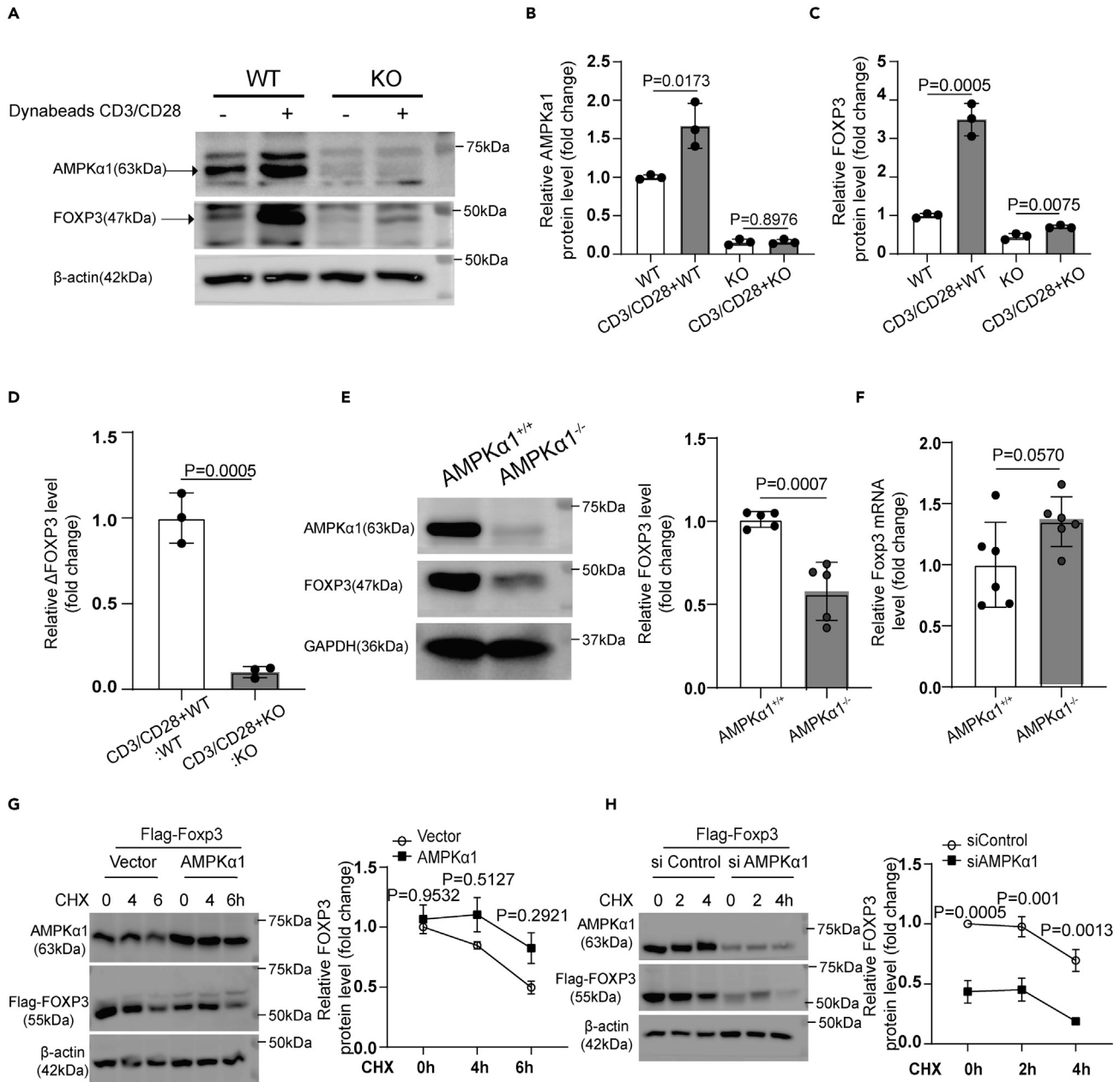


**Figure 5. AMPK $\alpha$ 1 maintains the protein stability of FOXP3**

(A) Isolated primary Treg cells (CD4+YFP+) from AMPK $\alpha$ 1<sup>Treg+/+</sup> (WT) and AMPK $\alpha$ 1<sup>Treg-/-</sup> (KO) mice were treated with Dynabeads CD3/CD28 beads at 1:1 ratio for 24 h. The expression of AMPK $\alpha$ 1 and FOXP3 were detected by Western blot.

(B) Quantification of relative AMPK $\alpha$ 1 expression in Treg cells from AMPK $\alpha$ 1<sup>Treg+/+</sup> (WT) and AMPK $\alpha$ 1<sup>Treg-/-</sup> (KO) mice stimulated with or without Dynabeads CD3/CD28 (n = 3 in each group; data are presented as individual values and mean  $\pm$  SD and analyzed by Student's t test).

(C) Quantification of relative FOXP3 expression in Treg cells from AMPK $\alpha$ 1<sup>Treg+/+</sup> (WT) and AMPK $\alpha$ 1<sup>Treg-/-</sup> (KO) mice stimulated with or without Dynabeads CD3/CD28 (n = 3 in each group; data are presented as individual values and mean  $\pm$  SD and analyzed by Student's t test).

(D) Quantification of the increased FOXP3 level ( $\Delta$ Foxp3) after CD3/CD28 treatment between Treg cells from AMPK $\alpha$ 1<sup>Treg+/+</sup> (WT) and AMPK $\alpha$ 1<sup>Treg-/-</sup> (KO) mice (n = 3 in each group; data are presented as individual values and mean  $\pm$  SD and analyzed by Student's t test).

(E) Representative Western blot and quantification of FOXP3 protein levels in AMPK $\alpha$ 1<sup>+/+</sup> and AMPK $\alpha$ 1<sup>-/-</sup> Tregs (n = 5 in each group; data are presented as individual values and mean  $\pm$  SD and analyzed by Student's t test).

(F) Quantification of relative *Foxp3* mRNA levels in AMPK $\alpha$ 1<sup>+/+</sup> and AMPK $\alpha$ 1<sup>Treg-/-</sup> Tregs (n = 6 in each group; data are presented as individual values and mean  $\pm$  SD and analyzed by Student's t test).

**Figure 5. Continued**

(G) Western blot and quantitative analysis of relative FOXP3 protein levels in HEK293T cells treated with cycloheximide (CHX) in combination with control vector or AMPK $\alpha$ 1 plasmid (n = 3 in each group/time point; data are presented as mean  $\pm$  SEM and analyzed by two-way ANOVA).

(H) Western blot and quantitative analysis of relative FOXP3 protein levels in HEK293T cells treated with CHX in combination with siControl or siAMPK $\alpha$ 1 (n = 3 in each group/time point; data are presented as mean  $\pm$  SEM and analyzed by two-way ANOVA).

AMPK in tumor-infiltrating Treg cells are largely unknown. Our results show that AMPK upregulation in tumor-infiltrating Treg cells prevents antitumor T cell response and thus promotes tumor progression, suggesting that specific inhibition of AMPK signaling in Treg cells might have therapeutic value for cancer treatment.

Our results support AMPK $\alpha$ 1 is required for FOXP3 protein stability and functional integrity of Treg cells in TME. Consistently with our observations, Michalek et al. reported showed that p-AMPK expression was higher in Treg cells than in conventional T cells, and that AMPK activation promoted the generation of Treg cells *in vivo* by regulating fatty acid oxidation (FAO) (Michalek et al., 2011). Consistent with these findings, pioglitazone and metformin were shown to enhance Treg cell expansion and inhibit the progression of plaque instability and autoimmune encephalomyelitis through activation of AMPK signaling (Sun et al., 2016; Tian et al., 2017). By contrast, other studies showed that absence of AMPK $\alpha$ 1 and AMPK $\alpha$ 2 had only a mild impact on immune homeostasis and the survival of Treg cells (Yang et al., 2017; Timilshina et al., 2019). The discrepancy between our results and the previous results might be because of different animal models, as the previous studies were mainly focused on the autoimmune disease caused by LKB1 and used very young mice in steady state. In addition, recent studies showed that SREBPs or CoREST (REST corepressor 1) deletion in Treg cells could promote antitumor effects while having limited impacts on immune homeostasis in steady state (Lim et al., 2021; Xiong et al., 2020), which matches the heterogeneous results regarding AMPK deletion. The role of AMPK in Treg cells warrants further investigation.

Stabilization of Foxp3 maintains Treg lineage plasticity and hampers the antitumor immune response (Martin et al., 2010). Uncovering the fundamental regulators that control Foxp3 expression is therefore essential for understanding and exploiting efficient Treg therapies for cancer treatment (Cortez et al., 2020). Loss of Foxp3 expression transforms Treg cells into so-called ex-Treg cells, which have no immunosuppressive ability but acquire effector Th cell-like phenotypes (Hori, 2014). This has potential clinical relevance, because the accumulation of ex-Treg cells in the TME potentiates immunotherapy (Hatzioannou et al., 2020; Li et al., 2020). The decreased FOXP3 protein stability and normal Foxp3 gene induction observed in AMPK $\alpha$ 1-deficient Treg cells in our study is not fully in accordance with the phenotype of ex-Treg cells; however, impaired FOXP3 protein stability without impairment of Foxp3 gene expression was also shown to impair Treg lineage stability and promote ex-Treg transformation in one recent study (Liu et al., 2019). It would therefore be interesting to investigate the effect of AMPK $\alpha$ 1 deficiency on ex-Treg transformation by crossing *Prkaa1<sup>fl/fl</sup>* mice with Treg lineage-tracking *Foxp3<sup>RES-YFP-Cre-Rosa26-loxp-td-RFP-loxp</sup>* mice (Gaddis et al., 2018). Fragility of Treg cells in TME was shown to promote antitumor immunity which potentiates the therapeutic effects of immune checkpoint therapy (Hatzioannou et al., 2020; Lim et al., 2021). However, the intracellular mechanism through which intratumoral Treg cells prevent fragile IFN- $\gamma$ -expressing Treg cells in TME remains largely unknown. Our findings demonstrate an essential role of AMPK in the prevention of induction of fragile Treg cells during tumor development.

FOXP3 ubiquitination and Treg function are tightly regulated by the E3 ubiquitin ligase CHIP (*STUB1*) (Chen et al., 2013). We found that AMPK $\alpha$ 1 deficiency upregulated CHIP expression in Treg cells *in vivo* and *in vitro*; however, the increased CHIP expression in tumors of AMPK $\alpha$ 1<sup>Treg<sup>-/-</sup></sup> mice was not confined to Foxp3<sup>+</sup> Treg cells but also appeared in non-Treg cells. A previous study showed that CHIP transcription and expression were tightly correlated with inflammatory cytokines (Chen et al., 2013). Therefore, we hypothesize that the increased CHIP expression in non-Treg cells in our experiments was because of the strong inflammatory conditions in the tumors of the AMPK $\alpha$ 1<sup>Treg<sup>-/-</sup></sup> mice. In addition to inflammatory cytokines, CHIP transcription is linked to different stresses such as heat shock and oxidative damages (Chen et al., 2013; Paul and Ghosh, 2014; Stankowski et al., 2011). Because of the crucial role of AMPK in oxidative stress regulation, the upregulation of CHIP in AMPK $\alpha$ 1-deficient Treg cells might be because of increased oxidative stress (Ren et al., 2020). Some post-translational modifications were also reported to regulate the expression or activity of CHIP (Paul and Ghosh, 2014; Zemanovic et al., 2018). Furthermore, one previous study showed a direct association between CHIP and AMPK levels in cardiomyocytes (Schisler et al., 2013), suggesting that another possible mechanism of CHIP regulation is direct phosphorylation of CHIP

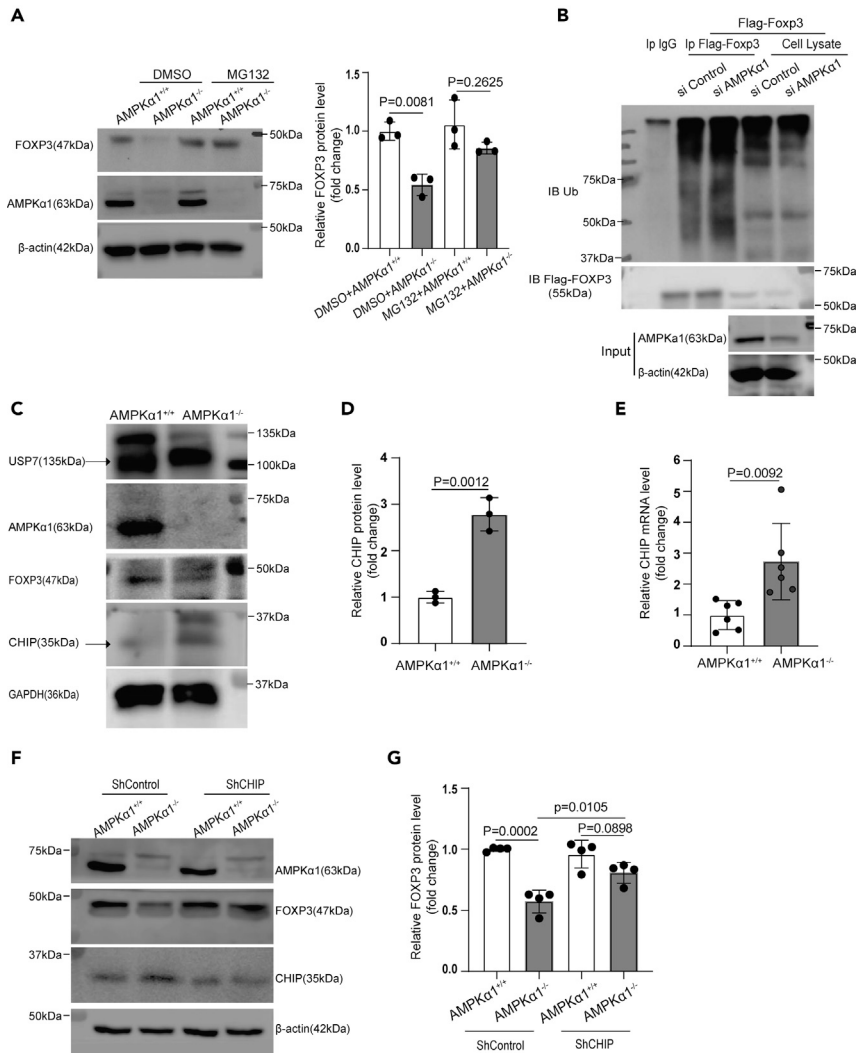


**Figure 6. Deficiency of AMPK $\alpha$ 1 promotes FOXP3 degradation through E3 ligase CHIP**

(A) Western blot and quantitative analysis of FOXP3 in AMPK $\alpha$ 1-sufficient (AMPK $\alpha$ 1<sup>+/+</sup>) and AMPK $\alpha$ 1-deficient (AMPK $\alpha$ 1<sup>Treg-/-</sup>) Treg cells (CD4<sup>+</sup>YFP<sup>+</sup>) in the presence or absence of proteasome inhibitor MG132 (n = 3 in each group; data are presented as individual values and mean  $\pm$  SD and analyzed by Student's t test).

(B) Effect of AMPK $\alpha$ 1 knockdown on FOXP3 ubiquitination. Flag-Foxp3 together with siControl or siAMPK $\alpha$ 1 was transfected into HEK293T cells. The cells were then treated with 5  $\mu$ M MG132 for 4 h before harvest and lysis. Ubiquitination of FOXP3 proteins was detected by Western blot.

(C) Western blot analysis of AMPK $\alpha$ 1, USP7, CHIP, and FOXP3 protein levels in sorted AMPK $\alpha$ 1-sufficient (AMPK $\alpha$ 1<sup>Treg+/+</sup>) and AMPK $\alpha$ 1-deficient (AMPK $\alpha$ 1<sup>Treg-/-</sup>) Treg cells (CD4<sup>+</sup>YFP<sup>+</sup>).

(D) Quantification of relative CHIP expression in sorted AMPK $\alpha$ 1-sufficient (AMPK $\alpha$ 1<sup>Treg+/+</sup>) and AMPK $\alpha$ 1-deficient (AMPK $\alpha$ 1<sup>Treg-/-</sup>) Treg cells (CD4<sup>+</sup>YFP<sup>+</sup>) (n = 3 in each group; data are presented as individual values and mean  $\pm$  SD and analyzed by Student's t test).

(E) Quantification of relative CHIP mRNA levels in sorted AMPK $\alpha$ 1-sufficient (AMPK $\alpha$ 1<sup>Treg+/+</sup>) and AMPK $\alpha$ 1-deficient (AMPK $\alpha$ 1<sup>Treg-/-</sup>) Treg cells (CD4<sup>+</sup>YFP<sup>+</sup>) (n = 6 in each group; data are presented as individual values and mean  $\pm$  SD and analyzed by Student's t test).

(F) Western blot analysis of FOXP3 protein levels in AMPK $\alpha$ 1-sufficient (AMPK $\alpha$ 1<sup>Treg+/+</sup>) and AMPK $\alpha$ 1-deficient (AMPK $\alpha$ 1<sup>Treg-/-</sup>) Treg cells (CD4<sup>+</sup>YFP<sup>+</sup>) in the presence of shControl lentivirus or shCHIP lentivirus.

(G) Quantification of relative FOXP3 expression in AMPK $\alpha$ 1-sufficient (AMPK $\alpha$ 1<sup>Treg+/+</sup>) and AMPK $\alpha$ 1-deficient (AMPK $\alpha$ 1<sup>Treg-/-</sup>) Treg cells (CD4<sup>+</sup>YFP<sup>+</sup>) in the presence of shControl or shCHIP lentivirus (n = 4 in each group; data are presented as individual values and mean  $\pm$  SD and analyzed by Student's t test).

by AMPK. Although the E3 ligase function of CHIP is well known, the mechanism by which CHIP itself is regulated is much less clear. Further experiments are needed to determine how AMPK regulates CHIP in Treg cells.

In conclusion, AMPK $\alpha$ 1 is a critical mediator controlling FOXP3 stability and the functional integrity of Treg cells in TME. Further studies are warranted to investigate whether therapeutic inhibition of AMPK activity in Treg cells bolsters antitumor immunity.

### Limitation of the study

In this study, we showed that AMPK $\alpha$ 1 promotes tumor development through elevation of the protein stability of Foxp3 in Treg cells. Mechanistically, AMPK $\alpha$ 1 downregulates CHIP, a well-known E3 ligase of Foxp3 which prevents Foxp3 ubiquitination and degradation. However, this specific mechanism on how AMPK regulates CHIP expression in Treg cells still lacks exploitation. It is meaningful to further investigate the detailed mechanism on how AMPK regulates CHIP expression in Treg cells. In addition, the exploitation of AMPK's role in Treg cells in clinical value needs to be further studied.

### STAR★METHODS

Detailed methods are provided in the online version of this paper and include the following:

- KEY RESOURCES TABLE
- RESOURCE AVAILABILITY
  - Lead contact
  - Materials availability
  - Data and code availability
- EXPERIMENTAL MODEL AND SUBJECT DETAILS
  - Cell lines
  - Mouse strains
  - Tumor models
- METHOD DETAILS
  - Cell isolation from tumors and lymphoid organs
  - Flow cytometry
  - Histopathology and immunofluorescent staining
  - Cell purification and culture
  - RNA extraction and qRT-PCR
  - Western blot analysis
  - Immunoprecipitation
  - Lentiviral shRNA transduction
- QUANTIFICATION AND STATISTICAL ANALYSIS

### SUPPLEMENTAL INFORMATION

Supplemental information can be found online at <https://doi.org/10.1016/j.isci.2021.103570>.

### ACKNOWLEDGMENTS

This study was supported by the National Institutes of Health grants (HL140954) (to P.S. and M.-H. Z.) and CA213022 and National Cancer Institute (CA213022) (to M.-H. Z.).

### AUTHOR CONTRIBUTIONS

J.A., P.S., and M.-H.Z. designed the experiments. J.A., C.Y., J.L., and S.Y. carried out all the experiments. J.A. and P.S. wrote the manuscript and prepared figures and tables. Z.L. constructed the pCHD1-Flag-SBP-Foxp3 plasmid. J.A., Y.D., Z.L., and S.Y., analyzed the data. M.-H.Z. conceived the project and revised the manuscript. All authors had final approval of the submitted and published version.

### DECLARATION OF INTERESTS

The authors declare no conflicts of interest.

Received: July 8, 2021  
Revised: November 2, 2021  
Accepted: December 2, 2021  
Published: January 21, 2022

## REFERENCES

- Bacchetta, R., Barzaghi, F., and Roncarolo, M.G. (2018). From IPEX syndrome to FOXP3 mutation: A lesson on immune dysregulation. *Ann. N. Y. Acad. Sci.* 1417, 5–22.
- Barbi, J., Pardoll, D.M., and Pan, F. (2015). Ubiquitin-dependent regulation of Foxp3 and Treg function. *Immunol. Rev.* 266, 27–45.
- Bennett, C.L., Christie, J., Ramsdell, F., Brunkow, M.E., Ferguson, P.J., Whitesell, L., Kelly, T.E., Saulsbury, F.T., Chance, P.F., and Ochs, H.D. (2001). The immune dysregulation, polyendocrinopathy, enteropathy, X-linked syndrome (IPEX) is caused by mutations of FOXP3. *Nat. Genet.* 27, 20–21.
- Bonney, K.M., Taylor, J.M., Thorp, E.B., Epting, C.L., and Engman, D.M. (2015). Depletion of regulatory T cells decreases cardiac parasitosis and inflammation in experimental Chagas disease. *Parasitol. Res.* 114, 1167–1178.
- Borst, J., Ahrends, T., Babala, N., Melief, C.J.M., and Kastenmuller, W. (2018). CD4(+) T cell help in cancer immunology and immunotherapy. *Nat. Rev. Immunol.* 18, 635–647.
- Carey, T.E., Takahashi, T., Resnick, L.A., Oettgen, H.F., and Old, L.J. (1976). Cell surface antigens of human malignant melanoma: mixed hemadsorption assays for humoral immunity to cultured autologous melanoma cells. *Proc. Natl. Acad. Sci. U S A.* 73, 3278–3282.
- Cha, J.H., Yang, W.H., Xia, W., Wei, Y., Chan, L.C., Lim, S.O., Li, C.W., Kim, T., Chang, S.S., Lee, H.H., et al. (2018). Metformin promotes antitumor immunity via endoplasmic-reticulum-associated degradation of PD-L1. *Mol. Cell* 71, 606–620 e7.
- Chen, Z., Barbi, J., Bu, S., Yang, H.Y., Li, Z., Gao, Y., Jinasena, D., Fu, J., Lin, F., Chen, C., et al. (2013). The ubiquitin ligase Stub1 negatively modulates regulatory T cell suppressive activity by promoting degradation of the transcription factor Foxp3. *Immunity* 39, 272–285.
- Cortez, J.T., Montauti, E., Shifrut, E., Gatchalian, J., Zhang, Y., Shaked, O., Xu, Y., Roth, T.L., Simeonov, D.R., Zhang, Y., et al. (2020). CRISPR screen in regulatory T cells reveals modulators of Foxp3. *Nature* 582, 416–420.
- Eichner, L.J., Brun, S.N., Herzig, S., Young, N.P., Curtis, S.D., Shackelford, D.B., Shokhirev, M.N., Leblanc, M., Vera, L.I., Hutchins, A., et al. (2019). Genetic analysis reveals AMPK is required to support tumor growth in murine Kras-dependent lung cancer models. *Cell Metab* 29, 285–302 e7.
- Faubert, B., Boily, G., Izreig, S., Griss, T., Samborska, B., Dong, Z., Dupuy, F., Chambers, C., Fuerth, B.J., Viollet, B., et al. (2013). AMPK is a negative regulator of the Warburg effect and suppresses tumor growth in vivo. *Cell Metab* 17, 113–124.
- Fontenot, J.D., Gavin, M.A., and Rudensky, A.Y. (2003). Foxp3 programs the development and function of CD4<sup>+</sup>CD25<sup>+</sup> regulatory T cells. *Nat. Immunol.* 4, 330–336.
- Gaddis, D.E., Padgett, L.E., Wu, R., McSkimming, C., Romines, V., Taylor, A.M., McNamara, C.A., Kronenberg, M., Crotty, S., Thomas, M.J., et al. (2018). Apolipoprotein AI prevents regulatory to follicular helper T cell switching during atherosclerosis. *Nat. Commun.* 9, 1095.
- Gutierrez-Salmeron, M., Garcia-Martinez, J.M., Martinez-Useros, J., Fernandez-Acenero, M.J., Viollet, B., Olivier, S., Chauhan, J., Lucena, S.R., De la Vieja, A., Goding, C.R., et al. (2020). Paradoxical activation of AMPK by glucose drives selective EP300 activity in colorectal cancer. *PLoS Biol.* 18, e3000732.
- Han, Y., Liu, D., and Li, L. (2020). PD-1/PD-L1 pathway: Current researches in cancer. *Am. J. Cancer Res.* 10, 727–742.
- Hao, Z., Ma, Y., Wang, J., Fan, D., Han, C., Wang, Y., Ji, Y., and Wen, S. (2015). Hypoxia promotes AMP-activated protein kinase (AMPK) and induces apoptosis in mouse osteoblasts. *Int. J. Clin. Exp. Pathol.* 8, 4892–4902.
- Hardie, D.G. (2015). Molecular pathways: Is AMPK a friend or a foe in cancer? *Clin. Cancer Res.* 21, 3836–3840.
- Hatzioannou, A., Alissafi, T., and Verginis, P. (2017). Myeloid-derived suppressor cells and T regulatory cells in tumors: Unraveling the dark side of the force. *J. Leukoc. Biol.* 102, 407–421.
- Hatzioannou, A., Banos, A., Sakelaropoulos, T., Fedonidis, C., Vidali, M.S., Kohne, M., Handler, K., Boon, L., Henriques, A., Koliarakis, V., et al. (2020). An intrinsic role of IL-33 in Treg cell-mediated tumor immunoevasion. *Nat. Immunol.* 21, 75–85.
- Herzig, S., and Shaw, R.J. (2018). AMPK: Guardian of metabolism and mitochondrial homeostasis. *Nat. Rev. Mol. Cell Biol* 19, 121–135.
- Hori, S. (2014). Lineage stability and phenotypic plasticity of Foxp3(+) regulatory T cells. *Immunol. Rev.* 259, 159–172.
- Kumar, V., Patel, S., Tcyganov, E., and Gabrilovich, D.I. (2016). The nature of myeloid-derived suppressor cells in the tumor microenvironment. *Trends Immunol.* 37, 208–220.
- Lee, Y.T., Lim, S.H., Lee, B., Kang, I., and Yeo, E.J. (2019). Compound C inhibits B16-F1 tumor growth in a syngeneic mouse model via the blockage of cell cycle progression and angiogenesis. *Cancers (Basel)* 11, 823.
- Li, C., Jiang, P., Wei, S., Xu, X., and Wang, J. (2020). Regulatory T cells in tumor microenvironment: New mechanisms, potential therapeutic strategies and future prospects. *Mol. Cancer* 19, 116.
- Lim, S.A., Wei, J., Nguyen, T.M., Shi, H., Su, W., Palacios, G., Dhungana, Y., Chapman, N.M., Long, L., Saravia, J., et al. (2021). Lipid signalling enforces functional specialization of Treg cells in tumours. *Nature* 591, 306–311.
- Liu, B., Salgado, O.C., Singh, S., Hippen, K.L., Maynard, J.C., Burlingame, A.L., Ball, L.E., Blazar, B.R., Farrar, M.A., Hoggquist, K.A., and Ruan, H.B. (2019). The lineage stability and suppressive program of regulatory T cells require protein O-GlcNAcylation. *Nat. Commun.* 10, 354.
- Martin, F., Ladoire, S., Mignot, G., Apetoh, L., and Ghiringhelli, F. (2010). Human FOXP3 and cancer. *Oncogene* 29, 4121–4129.
- Mayer, A., Denanglaire, S., Viollet, B., Leo, O., and Andris, F. (2008). AMP-activated protein kinase regulates lymphocyte responses to metabolic stress but is largely dispensable for immune cell development and function. *Eur. J. Immunol.* 38, 948–956.
- Michalek, R.D., Gerriets, V.A., Jacobs, S.R., Macintyre, A.N., MacIver, N.J., Mason, E.F., Sullivan, S.A., Nichols, A.G., and Rathmell, J.C. (2011). Cutting edge: Distinct glycolytic and lipid oxidative metabolic programs are essential for effector and regulatory CD4<sup>+</sup> T cell subsets. *J. Immunol.* 186, 3299–3303.
- Ohue, Y., and Nishikawa, H. (2019). Regulatory T (Treg) cells in cancer: Can Treg cells be a new therapeutic target? *Cancer Sci.* 110, 2080–2089.
- Ono, M. (2020). Control of regulatory T-cell differentiation and function by T-cell receptor signalling and Foxp3 transcription factor complexes. *Immunology* 160, 24–37.
- Overacre-Delgoffe, A.E., Chikina, M., Dadey, R.E., Yano, H., Brunazzi, E.A., Shayan, G., Horne, W., Moskovitz, J.M., Kolls, J.K., Sander, C., et al. (2017). Interferon-gamma drives Treg fragility to promote anti-tumor immunity. *Cell* 169, 1130–1141, e11.
- Overacre-Delgoffe, A.E., and Vignali, D.A.A. (2018). Treg fragility: A prerequisite for effective antitumor immunity? *Cancer Immunol. Res.* 6, 882–887.
- Paul, I., and Ghosh, M.K. (2014). The E3 ligase CHIP: Insights into its structure and regulation. *Biomed. Res. Int.* 2014, 918183.
- Petty, A.J., and Yang, Y. (2017). Tumor-associated macrophages: Implications in cancer immunotherapy. *Immunotherapy* 9, 289–302.
- Ren, H., Shao, Y., Wu, C., Ma, X., Lv, C., and Wang, Q. (2020). Metformin alleviates oxidative stress and enhances autophagy in diabetic kidney disease via AMPK/SIRT1-FoxO1 pathway. *Mol. Cell Endocrinol* 500, 110628.
- Schisler, J.C., Rubel, C.E., Zhang, C., Lockyer, P., Cyr, D.M., and Patterson, C. (2013). CHIP protects

- against cardiac pressure overload through regulation of AMPK. *J. Clin. Invest* 123, 3588–3599.
- Smigiel, K.S., Srivastava, S., Stolley, J.M., and Campbell, D.J. (2014). Regulatory T-cell homeostasis: Steady-state maintenance and modulation during inflammation. *Immunol. Rev.* 259, 40–59.
- Stankowski, J.N., Zeiger, S.L., Cohen, E.L., DeFranco, D.B., Cai, J., and McLaughlin, B. (2011). C-terminus of heat shock cognate 70 interacting protein increases following stroke and impairs survival against acute oxidative stress. *Antioxid. Redox Signal* 14, 1787–1801.
- Steinberg, G.R., and Carling, D. (2019). AMP-activated protein kinase: The current landscape for drug development. *Nat. Rev. Drug Discov.* 18, 527–551.
- Sun, Y., Tian, T., Gao, J., Liu, X., Hou, H., Cao, R., Li, B., Quan, M., and Guo, L. (2016). Metformin ameliorates the development of experimental autoimmune encephalomyelitis by regulating T helper 17 and regulatory T cells in mice. *J. Neuroimmunol.* 292, 58–67.
- Tamas, P., Hawley, S.A., Clarke, R.G., Mustard, K.J., Green, K., Hardie, D.G., and Cantrell, D.A. (2006). Regulation of the energy sensor AMP-activated protein kinase by antigen receptor and  $Ca^{2+}$  in T lymphocytes. *J. Exp. Med.* 203, 1665–1670.
- Tanaka, A., and Sakaguchi, S. (2017). Regulatory T cells in cancer immunotherapy. *Cell Res* 27, 109–118.
- Tian, Y., Chen, T., Wu, Y., Yang, L., Wang, L., Fan, X., Zhang, W., Feng, J., Yu, H., Yang, Y., et al. (2017). Pioglitazone stabilizes atherosclerotic plaque by regulating the Th17/Treg balance in AMPK-dependent mechanisms. *Cardiovasc. Diabetol.* 16, 140.
- Timilshina, M., You, Z., Lacher, S.M., Acharya, S., Jiang, L., Kang, Y., Kim, J.A., Chang, H.W., Kim, K.J., Park, B., et al. (2019). Activation of mevalonate pathway via LKB1 is essential for stability of Treg cells. *Cell Rep* 27, 2948–2961 e7.
- Trillo-Tinoco, J., Sierra, R.A., Mohamed, E., Cao, Y., de Mingo-Pulido, A., Gilvary, D.L., Anadon, C.M., Costich, T.L., Wei, S., Flores, E.R., et al. (2019). AMPK alpha-1 intrinsically regulates the function and differentiation of tumor myeloid-derived suppressor cells. *Cancer Res.* 79, 5034–5047.
- van Loosdregt, J., Fleskens, V., Fu, J., Brenkman, A.B., Bekker, C.P., Pals, C.E., Meering, J., Berkers, C.R., Barbi, J., Grone, A., et al. (2013). Stabilization of the transcription factor Foxp3 by the deubiquitinase USP7 increases Treg-cell-suppressive capacity. *Immunity* 39, 259–271.
- Veiga-Parga, T., Sehwat, S., and Rouse, B.T. (2013). Role of regulatory T cells during virus infection. *Immunol. Rev.* 255, 182–196.
- Wang, S., Liu, R., Yu, Q., Dong, L., Bi, Y., and Liu, G. (2019). Metabolic reprogramming of macrophages during infections and cancer. *Cancer Lett.* 452, 14–22.
- Watson, M.J., Vignali, P.D.A., Mullett, S.J., Overacre-Delgoffe, A.E., Peralta, R.M., Grebinoski, S., Menk, A.V., Rittenhouse, N.L., DePeaux, K., Whetstone, R.D., et al. (2021). Metabolic support of tumour-infiltrating regulatory T cells by lactic acid. *Nature* 591, 645–651.
- Wing, J.B., Tanaka, A., and Sakaguchi, S. (2019). Human FOXP3(+) regulatory T cell heterogeneity and function in autoimmunity and cancer. *Immunity* 50, 302–316.
- Xiong, Y., Wang, L., Di Giorgio, E., Akimova, T., Beier, U.H., Han, R., Trevisanut, M., Kalin, J.H., Cole, P.A., and Hancock, W.W. (2020). Inhibiting the coregulator CoREST impairs Foxp3<sup>+</sup> Treg function and promotes antitumor immunity. *J. Clin. Invest* 130, 1830–1842.
- Xu, F., Cui, W.Q., Wei, Y., Cui, J., Qiu, J., Hu, L.L., Gong, W.Y., Dong, J.C., and Liu, B.J. (2018). Astragaloside IV inhibits lung cancer progression and metastasis by modulating macrophage polarization through AMPK signaling. *J. Exp. Clin. Cancer Res.* 37, 207.
- Yang, J., Wei, P., Barbi, J., Huang, Q., Yang, E., Bai, Y., Nie, J., Gao, Y., Tao, J., Lu, Y., et al. (2020). The deubiquitinase USP44 promotes Treg function during inflammation by preventing FOXP3 degradation. *EMBO Rep.* 21, e50308.
- Yang, K., Blanco, D.B., Neale, G., Vogel, P., Avila, J., Clish, C.B., Wu, C., Shrestha, S., Rankin, S., Long, L., et al. (2017). Homeostatic control of metabolic and functional fitness of Treg cells by LKB1 signalling. *Nature* 548, 602–606.
- Yuan, X.L., Chen, L., Li, M.X., Dong, P., Xue, J., Wang, J., Zhang, T.T., Wang, X.A., Zhang, F.M., Ge, H.L., et al. (2010). Elevated expression of Foxp3 in tumor-infiltrating Treg cells suppresses T-cell proliferation and contributes to gastric cancer progression in a COX-2-dependent manner. *Clin. Immunol.* 134, 277–288.
- Zappasodi, R., Serganova, I., Cohen, I.J., Maeda, M., Shindo, M., Senbabaoglu, Y., Watson, M.J., Leftin, A., Maniyar, R., Verma, S., et al. (2021). CTLA-4 blockade drives loss of Treg stability in glycolysis-low tumours. *Nature* 591, 652–658.
- Zemanovic, S., Ivanov, M.V., Ivanova, L.V., Bhatnagar, A., Michalkiewicz, T., Teng, R.J., Kumar, S., Rathore, R., Pritchard, K.A., Jr., Konduri, G.G., and Afolayan, A.J. (2018). Dynamic phosphorylation of the C terminus of Hsp70 regulates the mitochondrial import of SOD2 and redox balance. *Cell Rep.* 25, 2605–2616 e7.
- Zhang, Z., Li, F., Tian, Y., Cao, L., Gao, Q., Zhang, C., Zhang, K., Shen, C., Ping, Y., Maimela, N.R., et al. (2020). Metformin enhances the antitumor activity of CD8(+) T lymphocytes via the AMPK-miR-107-eomes-PD-1 pathway. *J. Immunol.* 204, 2575–2588.

**STAR★METHODS**

**KEY RESOURCES TABLE**

REAGENT or RESOURCE	SOURCE	IDENTIFIER
<i>Antibodies</i>		
Flow cytometry: PE anti-mouse CD45 antibody (30-F11)	BioLegend	103106; RRID: AB_312971
Flow cytometry: Pacific blue anti-mouse CD45 antibody (30-F11)	BioLegend	103126; RRID:AB_493535
Flow cytometry: Alexa Fluor 700 anti-mouse CD45 antibody (30-F11)	BioLegend	103128; RRID:AB_493715
Flow cytometry: Brilliant Violet 605™ anti-mouse CD3e antibody (17A2).	BioLegend	100237; RRID:AB_2562039
Flow cytometry: Pacific blue anti-mouse CD4 antibody (RM4-5)	BioLegend	100531; RRID:AB_493374
Flow cytometry: PE/Cyanine 7 anti-mouse CD4 antibody (GK1.5)	BioLegend	100422; RRID:AB_312707
Flow cytometry: Alexa Fluor 488 anti-mouse CD8a (53-6.7)	BioLegend	100723; RRID:AB_389304
Flow cytometry: Alexa Fluor 488 anti-mouse/rat/human Foxp3 antibody (150D)	BioLegend	320012; RRID:AB_439748
Flow cytometry: PE anti-mouse Foxp3 antibody (MF-14)	BioLegend	126404; RRID:AB_1089117
Flow cytometry: Alexa Fluor 488 anti-mouse Foxp3 antibody (MF-14)	BioLegend	126406; RRID:AB_1089114
Flow cytometry: Alexa Fluor 488 anti-GFP (FM264G)	BioLegend	338008; RRID:AB_2563288
Flow cytometry: PE anti-GFP(FM264G)	BioLegend	338004; RRID:AB_2650615
Flow cytometry: PE Rat anti-mouse CD25(3C7)	BioLegend	101904; RRID:AB_312847
Flow cytometry: PE CD278(iCOS) (15F9)	BioLegend	107705; RRID:AB_313334
Flow cytometry: PE anti-mouse IFN-γ(XMG1.2)	BioLegend	505808; RRID:AB_315402
Flow cytometry: PE-Cy7 anti-mouse CD357 (GITR) (YGITR 765)	BioLegend	120222; RRID:AB_528907
Flow cytometry: PE anti-mouse CD152 (CTLA-4) (UC10-4B9)	BioLegend	106305; RRID:AB_313254
Flow cytometry: PE anti-mouse CD279 (PD1) (RMP1-30)	BioLegend	109103; RRID:AB_313420
Flow cytometry: PE anti-mouse IL10 (JES5-16E3)	BioLegend	505008; RRID:AB_315362
Flow cytometry: PE anti-mouse CD304 (Nrp1) (3E12)	BioLegend	145204; RRID:AB_2561928
Western blot: Rabbit anti-FOXP3 antibody	abcam	Ab75763; RRID:AB_1310238
Western blot: FOXP3 Monoclonal Antibody (150D/E4)	eBioscience	14-4774-82; RRID:AB_467552
Immunofluorescence: FOXP3 (D608R) rabbit	Cell Signaling	12653S; RRID:AB_2797979
Flow cytometry/Western blot/ Immunohistochemistry: Recombinant anti-AMPK alpha 1 antibody	Abcam	ab32047; RRID:AB_722764

(Continued on next page)

**Continued**

REAGENT or RESOURCE	SOURCE	IDENTIFIER
Immunohistochemistry: Recombinant anti-AMPK alpha 1 antibody	Abcam	Ab110036; RRID:AB_10862578
Western blot: Goat AMPK $\alpha$ 1(C-20)	Santa Cruz	Sc-19128; RRID:AB_2268724
Immunofluorescence: CD3e Monoclonal antibody (SP7)	Thermo Fisher	MA5-14524; RRID:AB_10982026
Immunofluorescence: Recombinant anti-CD8 alpha antibody	Abcam	Ab217344; RRID:AB_2890649
Immunofluorescence: Recombinant anti-CD4 antibody	Abcam	Ab183685; RRID:AB_2686917
Immunofluorescence: CD31(PECAM-1) (D8V9E) Rabbit mAb	Cell signaling	77699; RRID:AB_2722705
Immunofluorescence: Recombinant anti-Ki-67 antibody (SP6)	Abcam	Ab16667; RRID:AB_302459
A Western blot: Anti $\beta$ -actin antibody(C4)	Santa Cruz	Sc-47778; RRID:AB_2714189
Western blot/Immunofluorescence: Anti-CHIP(Stub1) antibody	Santa Cruz	Sc-133066; RRID:AB_2286870
Western blot: Anti-HAUSP(USP7) antibody (H-12)	Santa Cruz	Sc-137008; RRID:AB_2214163
Western blot: Ubiquitin antibody	Cell signaling	3933; RRID:AB_2180538
Immunofluorescence:CD45R(B220) Monoclonal Antibody (RA3-6B2)	Thermo Fisher	14-0452-85; RRID:AB_467255
Flow cytometry/Immunofluorescence: Goat anti-Rabbit IgG H&L (Alexa Fluor 488)	abcam	Ab150077; RRID:AB_2630356

**Chemicals, peptides, and recombinant proteins**

Anti-CD3/CD28 Dynabeads	ThermoFisher	11452D
IL2 Recombinant Mouse Protein	ThermoFisher	PMC0025
Fixable Viability Dye eFluor 660	ThermoFisher	65-0864-18
Fixable Viability Dye eFluor 780	ThermoFisher	65-0865-14
Cycloheximide	SIGMA	01810
MG132	SIGMA	133407-82-6
DNase I	SIGMA	10104159001
Collagenase D	SIGMA	11088866001
iScript cDNA Synthesis Kit	BioRad	170-8891
Lipofectamine 2000 Transfection Reagent	ThermoFisher	11668019
Lipofectamine RNAiMAX Transfection Reagent	ThermoFisher	13778075
Albumin, Bovine Fraction V (BSA)	RPI	A30075-100;CAS:9048-46-8
Fetal bovine serum (FBS)	Sigma-Aidrich	12303C
Penicillin-Streptomycin	ThermoFisher	15140122
RPMI 1640	CORNING	10-040-CV
DMEM	CORNING	10-013-CV

**Critical commercial assays**

Dynabeads Mouse CD4+ CD25+ Treg isolation Kit	ThermoFisher	11463D
eBioscience Foxp3/Transcription Factor Staining Buffer Set	ThermoFisher	00-5523-00
eBioscience Protein Transport Inhibitor Cocktail (500x)	ThermoFisher	00-4980-03

(Continued on next page)

**Continued**

REAGENT or RESOURCE	SOURCE	IDENTIFIER
eBioscience Cell Stimulation Cocktail (500x)	ThermoFisher	00-4970-03
Dynabeads Untouched Mouse CD4 Cells Kit	ThermoFisher	11416D
Experimental models: Cell lines		
HEK 293T cells	ATCC	CRL-11268
B16F10 melanoma	ATCC	CRL-6475-LUC2™
LL/2(LLC1)	ATCC	CRL-1642
Experimental models: Organisms/strains		
Mouse: C57BL/6J	The Jackson Laboratory	JAX:000664
Mouse: Prkaa1 <sup>fl/fl</sup>	The Jackson Laboratory	JAX:014141
Mouse: Foxp3 <sup>YFP/Cre</sup>	The Jackson Laboratory	JAX:016959
Oligonucleotides		
See Table S1 for RT-PCR primers of <i>Foxp3</i> , <i>CHIP</i> , and <i>GAPDH</i>	This paper	NA
Recombinant DNA		
pCHD1-Flag-SBP-Foxp3	This paper	NA
CHIP(STUB1) shRNA(m) Lentiviral Particles	Santa Cruz	Sc-44731-V
Software and algorithms		
GraphPad Prism 8	GraphPad Software	<a href="https://www.graphpad.com/">https://www.graphpad.com/</a>
ImageJ Software	ImageJ	<a href="https://imagej.net/Welcome">https://imagej.net/Welcome</a>
FlowJo	FlowJo 7.6	<a href="https://www.flowjo.com/">https://www.flowjo.com/</a>

## RESOURCE AVAILABILITY

### Lead contact

Requests for further information and reagents may be directed to the lead contact, Ming-Hui Zou ([mzou@gsu.edu](mailto:mzou@gsu.edu)).

### Materials availability

Unique reagents generated in this study are available from the lead contact with a completed Material Transfer Agreement.

### Data and code availability

All data produced in this study are available from the lead contact upon request.

This paper has no original code.

Any additional information required to reanalyze the data showed in this paper is available from the lead Contact upon request.

## EXPERIMENTAL MODEL AND SUBJECT DETAILS

### Cell lines

HEK 293T cells, B16-F10-luc2 cells, and LLC cells were cultured in Dulbecco's Modification of Eagle's Medium (CORNING) containing 4.5 g/L glucose, L-glutamine, and sodium pyruvate, supplemented with 10% FBS, 100 U/ml penicillin, and 100 µg/ml streptomycin in a 37°C incubator with humidity and 5% CO<sub>2</sub>. Moreover, primary mouse cells were isolated from 6–8 mice/group on the same day.

### Mouse strains

Prkaa1<sup>fl/fl</sup>, Foxp3<sup>Cre/YFP</sup>, and C57BL/6 mice were purchased from Jackson Laboratory (Bar Harbor, ME). All genetic models had the C57BL/6 background. Prkaa1<sup>fl/fl</sup>Foxp3<sup>Cre/YFP</sup> mice were used at 10–16 weeks of age unless otherwise noted. Age-matched and sex-matched Prkaa1<sup>+/+</sup>Foxp3<sup>Cre/YFP</sup> mice were used as controls.

All mice were housed in specific pathogen-free conditions in the animal facilities at Georgia State University. The animal protocol was reviewed and approved by the Georgia State University Institutional Animal Care and Use Committee.

### Tumor models

B16-F10 murine melanoma cells and LLC cells were purchased from the ATCC. First, we confirmed that the cell lines were negative for Mycoplasma spp. We subcutaneously implanted 5x10<sup>5</sup> B16-F10 melanoma cells or 5x10<sup>5</sup> LLC cells on the backs of 10–12-week-old male AMPK $\alpha$ 1<sup>Treg+/+</sup> and AMPK $\alpha$ 1<sup>Treg-/-</sup> mice. The mice were monitored every day, and tumor growth and tumor size were determined based on tumor volume (0.5 x width<sup>2</sup> x length). Tumors were collected 10–13 days after inoculation unless otherwise noted.

## METHOD DETAILS

### Cell isolation from tumors and lymphoid organs

Tumor-infiltrating lymphocytes were isolated by incubating tumor tissues in collagenase D (1 mg/ml, Roche) and DNase I (0.25 mg/ml, Sigma) for one hour. Single-cell suspensions from tumors were generated by passing the digested tumor tissues through a 40- $\mu$ m cell strainer. Single-cell suspensions from spleen were obtained directly by passing the tissues through a 40- $\mu$ m cell strainer.

### Flow cytometry

Each reaction was performed with more than 1 x 10<sup>6</sup> cells, and a minimum of 1 x 10<sup>5</sup> events were recorded. Fluorescence-positive cells were analyzed with a FACScalibur or LSRFortessa device (Becton Dickinson, CA). Cells were processed for viability staining using eBioscience LIVE/DEAD fixable Dye eFluor 660 or eFluor 780 (ThermoFisher). For analysis of cell surface markers, cells were stained in stain buffer (BD bioscience) with the appropriate antibodies. Information on antibodies, clones, and fluorophores is provided in the [Key resources table](#). A Foxp3/transcription factor staining buffer set from eBioscience was used for intracellular staining. For staining intracellular cytokines, cells were stimulated for 6–18 h with a cell stimulation cocktail (ThermoFisher) conjunction with protein transport inhibitor cocktail (ThermoFisher) before being stained. After stimulation, the cells were stained with appropriate antibodies following the manufacturer's instructions. For YFP staining, Alexa Fluor 488 anti-GFP or PE anti-GFP antibody from BioLegend was used.

### Histopathology and immunofluorescent staining

Organs were fixed with 10% (v/v) neutral buffered formalin, embedded in paraffin, sectioned, and stained with hematoxylin and eosin. For immunofluorescent staining, 4- $\mu$ m sectioned paraffin slides were subjected to xylene and alcohol for dehydration. Then, the slides were subjected to antigen retrieval, permeabilized with 0.2% Triton X-100, and blocked with protein block goat serum (BioGenex, Fremont, CA). Then, the slides were incubated with CD31, anti-Ki67, Foxp3, CD3e, B220, CD4, CD8, or CHIP antibodies at 4°C overnight. Alexa Fluor 555 and Alexa Fluor 488 goat anti-rabbit, anti-rat, or anti-mouse were used as secondary antibodies, incubated at room temperature for one h. Cell nuclei were stained with DAPI and mounted with VectaMountTMAQ (#5501, Vector Laboratories) for fluorescence microscopy. Quantification was performed using Image J software.

### Cell purification and culture

Lymphocytes were isolated from spleens, CD4<sup>+</sup> T cells were isolated using a Dynabeads CD4<sup>+</sup> T cell Isolation Kit (ThermoFisher). Then, CD4<sup>+</sup>YFP<sup>+</sup> Treg cells were purified by YFP (GFP staining) using FACSAria II (BD Bioscience). The purified cells were cultured in RPMI 1640 supplemented with 10% FBS, 100 U/ml penicillin, 100 mg/ml streptomycin, and  $\beta$  mercaptoethanol.

### RNA extraction and qRT-PCR

According to the manufacturer's instructions, RNA was extracted using the RNeasy Mini Kit (QIAGEN, Hilden, Germany). cDNA was synthesized using the iScript cDNA Synthesis Kit. The expression of Foxp3 and CHIP mRNAs was determined by quantitative real-time PCR (qRT-PCR). Each cDNA sample was amplified using SYBR Green (Bio-rad, Hercules, CA) on a Bio-rad CFX96 Touch Real-time PCR detection system.

### Western blot analysis

Cells were lysed with NP-40 lysis buffer (1% NP-40, 20 mM Tris-HCl pH 7.5, 150 mM NaCl, 5 mM EDTA, 50 mM NaF, 2 mM Na<sub>3</sub>VO<sub>4</sub>, and 10 µg/ml each of aprotinin and leupeptin) or with 1× SDS sample buffer (50 mM Tris-HCl pH 6.8, 100 mM DTT, 2% SDS, and 10% glycerol). Proteins were separated by SDS-PAGE and transferred to nitrocellulose membranes (Millipore, Billerica, MA). Membranes were visualized with an enhanced chemiluminescence detection system (Thermo Fisher Scientific, Waltham, MA). When necessary, the membranes were stripped by incubation in stripping buffer (Thermo Fisher Scientific, Waltham, MA) for 15 - 30 min with constant agitation, washed, and then re-probed with various other antibodies.

### Immunoprecipitation

For immunoprecipitation, HEK293T cells were transfected with lipo2000 or RNA iMAX. Forty-eight hours after transfection, the cells were treated with MG132 for six h and then lysed in lysis buffer (50 mM Tris-HCl pH 7.5, 0.5% Nonidet p40 (US Biological), 1 mM EDTA and 40 mM NaCl with 1% protease inhibitor cocktail (ThermoFisher)). Anti-FLAG M2 affinity gel was used for immunoprecipitation. The precipitated samples were then boiled and analyzed by western blot.

### Lentiviral shRNA transduction

CHIP (Stub1) shRNA(m) lentiviral particles were obtained from Santa Cruz. Purified CD4<sup>+</sup>YFP<sup>+</sup> Treg cells were activated with Dynabeads CD3/CD28 plus IL-2 (200 U/ml) for 48 h and then transduced with lentivirus in the presence of 10 µg/ml polybrene by centrifugation at 900 g for 3 h. The transduced cells were then cultured in RPMI 1640 medium for 48 h and subsequently lysed for western blot analysis.

### QUANTIFICATION AND STATISTICAL ANALYSIS

All statistical analyses were performed using GraphPad Prism version 8 (GraphPad Software, CA). Student's t test was used for analysis comparing two samples. One-way ANOVA tested differences among multiple samples. Two-way ANOVA was applied to study the effect of two parameters (i.e., time and treatment) and their interaction.  $P < 0.05$  was considered statistically significant.